Mimicking the Natural Basement Membrane for Advanced Tissue Engineering

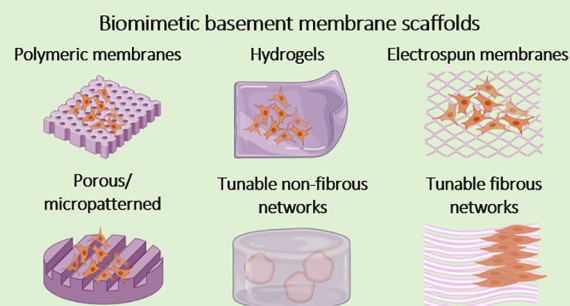Puja Jain, Sebastian Bernhard Rauer, Martin Möller, and Smriti Singh*

Read Online

ACCESS | Metrics & More | Article Recommendations

ABSTRACT: Advancements in the field of tissue engineering have led to the elucidation of physical and chemical characteristics of physiological basement membranes (BM) as specialized forms of the extracellular matrix. Efforts to recapitulate the intricate structure and biological composition of the BM have encountered various advancements due to its impact on cell fate, function, and regulation. More attention has been paid to synthesizing biocompatible and biofunctional fibrillar scaffolds that closely mimic the natural BM. Specific modifications in biomimetic BM have paved the way for the development of *in vitro* models like alveolar-capillary barrier, airway models, skin, blood-brain barrier, kidney barrier, and metastatic models, which can be used for personalized drug screening, understanding physiological and pathological pathways, and tissue implants. In this Review, we focus on the structure, composition, and functions of *in vivo* BM and the ongoing efforts to mimic it synthetically. Light has been shed on the advantages and limitations of various forms of biomimetic BM scaffolds including porous polymeric membranes, hydrogels, and electrospun membranes This Review further elaborates and justifies the significance of BM mimics in tissue engineering, in particular in the development of *in vitro* organ model systems.


Biomimetic basement membrane scaffolds
Polymeric membranes — Hydrogels — Electrospun membranes
Porous/micropatterned — Tunable non-fibrous networks — Tunable fibrous networks

INTRODUCTION

Cells reside in a tissue environment that is primarily composed of water, proteoglycans (glyocaminoglycans), and proteins, such as collagen, elastin, fibronectin, and laminin.[1] This noncellular microenvironment is termed as the extracellular matrix (ECM) and plays a major role in controlling cellular behavior, tissue formation, and homeostasis. There exists a variation in ECM at different tissue locations due to the different compositions, combinations, and arrangements of proteins and glycans that make up the ECM.[2] In 1857, the term basement membrane (BM) was first used by Robert Todd and William Bowman to describe the specialized ECM membrane on which epithelial cells rest as a "continuous basement membrane of excessive tenuity, apparently identical with that which supports the epithelium of mucous membranes".[3] The BM is located basolateral to the epithelial and endothelial cell layers and surrounds peripheral nerve axons, adipose, and muscle cells.[4] It is ubiquitous and forms a continuous sheath around all vital organs including the cardiovascular, nervous, respiratory, excretory, digestive, and integumentary systems,[5−14] as represented in Figure 1. Functionally, this dynamic structure is involved in regulating and maintaining biochemical signals between cells and their surrounding tissues, apart from providing physical support.[15−19] BMs also maintain organ shape and size and their significance is further observed in the development of diseases

due to genetic mutations in BM genes.[20] Mutations in genes that code for the collagen IV network including COL4A3, COL4A4, COL4A5 can lead to Alport Syndrome or thin BM nephropathy (TBMN) that affect the kidney filtration barrier.[21] Additionally, defects in genes coding CD151 are associated with defects in the glomerular BM, and defects in the Lmγ1 gene leads to embryonic death associated with nondeveloped BM.[22,23] Moreover, defects in BM regeneration or development have also been observed in cases of corneal stromal fibrosis and epidermolysis bullosa.[24,25]

The above-mentioned vital functions deem it necessary to design scaffolds that closely resemble the structural, mechanical, and functional characteristics of the native BM. Furthermore, the relevance of an appropriate scaffold design is described in a vast array of research that highlight the influence of biophysical and biochemical signals on cellular processes such as proliferation, migration, differentiation, and gene expression.[26−30] Scaffold biophysical cues include tensile
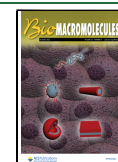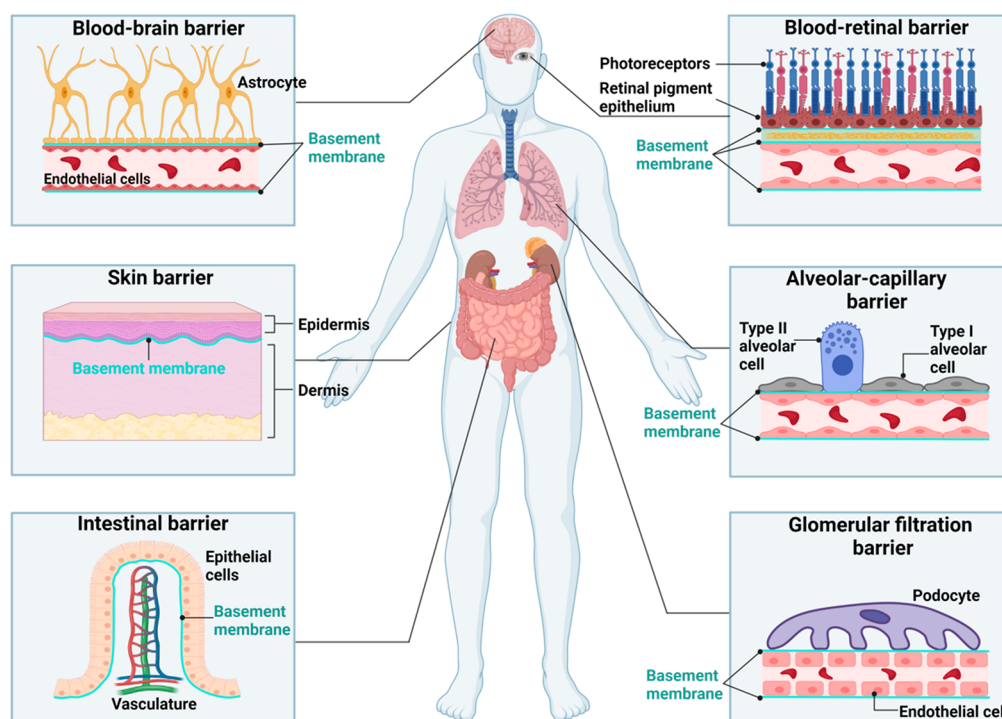
Figure 1. Basement membrane location: Basement membrane (BM) is ubiquitous in the human body and is located adjacent to the epithelium, endothelium, and parenchymal cells including muscle, adipose as well as nerve cells. It is involved in many vital physiological processes and is found in many organ barriers including the brain, retina, kidney, intestine, and lung. The schematic displays examples of some of the vital organs where the BM can be found. This includes the underlying areas of the epithelium and endothelium, where it supports and physically separates the different cellular layers. Created with Biorender.com

modulus, pore size, roughness, and topology, whereas biochemical cues include growth factors, cell adhesion ligands, hormones, and other molecules that influence cell behavior.[31] Discrepancies observed in the interaction of cells between fibers and flat hydrogel surfaces are highlighted in the works of Baker and colleagues.[32] Their experimental results, involving the interaction of NIH 3T3 fibroblast cells with methacrylated dextran (DexMa) in the form of electrospun fibers and hydrogel surfaces, implicate the sensitivity of cells toward the scaffold's architecture. An opposite behavior is observed on the fiber and hydrogel scaffolds where cell spreading is prominent on stiff hydrogels as compared with stiff fibers and vice versa. Similar differences in the expression of αSMA by endothelial cells on nonwoven electrospun meshes and PET membranes were observed by Jain et.al.[33] This illustrates the influence of scaffold structure and property on cell behavior when used to mimic ECM like materials such as the BM. Furthermore, Slater et al. demonstrated confluent monolayer formation of cells on the electrospun membranes as opposed to that on hydrogel systems with embedded adhesive ligands and Matrigel.[34]

To reach the goal of a native-like scaffold, a wide variety of different biomaterials have been synthesized and manufactured, which feature typical BM properties such as intricate fibrillar architecture, the viscoelastic mechanical properties, the adhesive sequences, the dynamic enzyme-induced nature as well as the possibility of controlled storage and release of bioactive substances such as growth factors.[33,35−43] These biomaterials are mostly fabricated from natural and synthetic polymer systems and try to combine multiple BM properties that are tailored toward the needs of a desired tissue construct or a region of interest.[44] Scaffolds are used to construct in vitro models that are valuable research tools for unraveling

fundamental biological processes involved in tissue homeostasis and disease development as well as serving as industrial platforms for drug screening.[5,6,8−14,45] Furthermore, despite the success of animal models as an invaluable source of scientific knowledge, animal models are often limited in translation to human biology and response.[46,47] Additionally, the three R's principle when conducting animal studies (reduction, replacement, and refinement) abide by animal ethics and do promote the use of other systems such as simulation or in vitro models when possible.[48,49] Therefore, the application of in vitro models and scaffolds might not only uncover scientific knowledge and save patient lives but also reduce the necessity of animal studies.

The importance of mimicking the BM has been highlighted in this Review by elaborating on its structure, assembly, function, and location in the human body. We provide the readers an understanding of the various forms of available BM mimics from naturally derived to synthetic materials as well as their strengths and weaknesses. This Review further aims to help understand key points required to construct appropriate BM scaffolds that closely represent their in vivo counterparts.

■ STRUCTURE AND ASSEMBLY OF NATURAL BM

The BM comprises basal lamina (subdivided into lamina lucida \rara and lamina densa) and the reticular lamina. Closer to the parenchymal cell layer with an average thickness of 27 nm is the lamina lucida, and underlying this layer, closer to the connective tissue, is the dense fibrillar lamina densa with an average thickness of 53 nm. The reticular lamina is observed to be structurally similar to the loose interconnective tissue. Recently, the basal lamina is also referred to as the BM and the words are used interchangeably.[50,51] BM is considered a thin
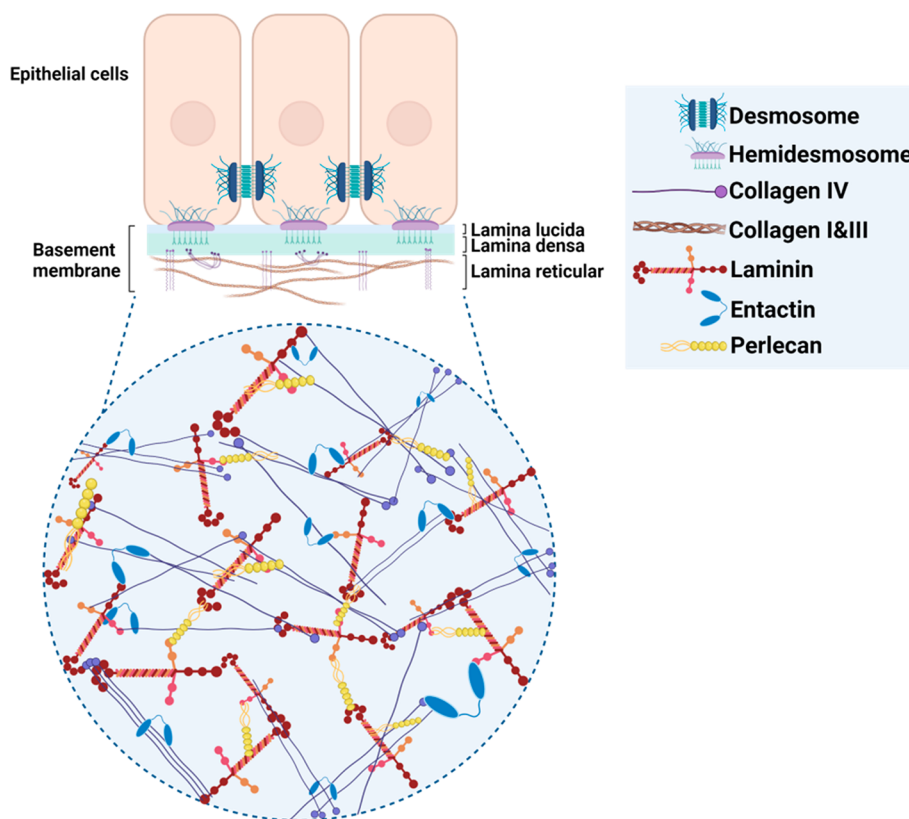
Figure 2. Structural feature of basement membrane: A dense fibrillar layer, primarily located underneath the epithelial cells, the lamina lucida, and densa together with the lamina reticular correspond to the basement membrane. At the molecular level, it is primarily composed of dynamic laminin and a network of collagen IV that are bound together by entactin (nidogen) along with perlecan to form a network of supporting ECM for cellular layers. Created with Biorender.com.

Table 1. Varying Components of Naturally Occurring BM Based on Tissue Location

tissue	collagen	laminin	nidogen	others	ref
blood-brain barrier BM	collagenIV	laminin211, laminin411, laminin511	nidogen-1, -2	perlecan, agrin, fibronectin	65
skin BM	collagenIV, collagenVII,	laminin511, laminin411, laminin322	nidogen-1, -2	perlecan, agrin, fibrillar	66
intestinal barrier BM	collagenIV	laminin111, laminin511, laminin332	nidogen-1, -2	perlecan, agrin, fibulin	67,68
corneal BM	collagenIV, collagenVII, collagenXII, collagenXVII, collagenXVIII,	laminin311, laminin333, laminin411, laminin511	nidogen-1, -2	perlecan, fibronectin	11
alveolar-capillary BM	collagenIV, collagenVIII	laminin411, laminin511	nidogen-1, -2	perlecan, agrin, fibronectin	69,70
glomerular BM	collagenIV	laminin221, laminin521	nidogen-1, -2	agrin	7,71

(50−300 nm) fibrillar layer resembling the ECM underlying the parenchymal cell layers that separate it from the connective tissue.[52,53]

Molecularly, BM is composed of varying combinations and isoforms of four principle biomolecules that include collagen IV, laminin, nidogen, and perlecan at various tissue locations (Figure 2).[54] Other molecules include agrin, fibronectin, fibrinogen, and collagen type XV and type XVIII.[55] The highly cross-linked collagen together with the more dynamic noncovalent laminin isoform network provides mechanical stability to the BM. Nidogen, also known as entactin, binds the collagen IV and laminin and also binds to perlecan, fibronectin, and fibrinogen.[56,57] Type IV collagen in mammals is a combination of 6 distinct α polypeptide chains (α1-α6). The α chains have three domains: amino-terminal 7S domain, a middle triple-helical domain (1400 amino acid), and a

noncollagenous carboxy-terminal globular domain (NC-1) (230 amino acid). Repetitive units of Gly-X-Y are found in the triple helical\collagen and 7S domains. The triple-helical domain has 22 interruptions that administer flexibility to it. The 6-α chains are 50−70% homologous at the amino acid level and differ in their NC1 domain. Cells produce collagen IV in the form of protomers (heterotrimers consisting of three α chain combinations). Different protomer combinations of collagen IV contribute to 50% of the BM found at different locations.[51,58,59] Laminin is a heterotrimeric protein derived from genes that code for α (1−5), β (1−3), and γ (1−3) chains. The average size of the α chain is 400 kDa, and β and γ are 200 kDa.[60] Constituting the second major component of the BM, the laminin isoforms (a combination of the different α, β, and γ chains) resemble a three-pronged-fork that stems from six domains of the chain. The C-terminal of the α, β, and

Table 2. Biophysical Properties of Naturally Occurring BM Vary Based on Species and Organ

species, tissue	Young's modulus [kPa]	ultimate tensile strength [MPa]	pore size [nm]	thickness [μm]	ref
human, anterior BM of cornea	7.5 ± 4.2	3.81 ± 0.4	92	<0.5	98,124
human, Descemet's membrane of cornea	50 ± 17.8	1.72 ± 0.19	38	>5	98,101
mouse, Matrigel	0.45	-	-	1000	100
cat, lens capsule BM	820	1.7	-	61	125
rabbit, anterior BM of the cornea	4.5 ± 1.2	3.83 ± 0.91	-	-	126,127
rabbit, renal tubule	500	0.5	-	0.26	128

γ chains form the handle (consist of I and II domains of each chain), whereas the N-termini short arms of the chains (consisting of III, IV, V, and VI domains of each chain) form the prongs.[61] Nidogen, also known as entactin, is a glycoprotein that makes up nearly 3% of the BM. Transcription of the genes NID1 and NID2 lead to the formation of Nidogen1 (30 nm long) and Nidogen2 (40 nm long) respectively.[62] The two forms are prevalent in the differently localized BM. Nidogen binds to collagen, laminin, fibronectin, and perlecan.[51,59,63] Perlecan is a 450 kDa heparan sulfate glycoprotein that is ubiquitous in the BM and has binding sites on collagen, nidogen, and laminin. Structurally perlecan consists of five domains (I–V) akin to a pearl on a string arrangement.[51,59,64]

The varying composition and isoforms of the above-mentioned components trigger specificity to the BM that is prevalent at its different anatomical locations, Table 1. Despite differences in molecular isoforms of the principle components at various tissue locations, they share a similar strategy of self-assembly.[56] Protomers of collagen IV and laminin hetero-trimers are assembled in the Golgi apparatus inside the cell along with other single molecules such as nidogen and perlecan. Secretory vesicles transport these molecules to the extracellular environment, where laminins assemble on the cell surface receptors via binding motifs. Secreted collagen IV protomers form networks with the assembled laminin through nidogen and perlecan.[55,56] The cascade of intracellular production and secretion followed by extracellular self-assembly leads to BM formation.

■ PROPERTIES AND FUNCTION OF THE NATURAL BM

Cells adhere to the underlying BM by an interaction between their receptor proteins such as integrins to adhesion motifs on the collagen and laminin networks, as seen in Figure 2.[1,72] It provides physical support to the overlying epithelial and endothelial tissues and also acts as an interface to the interstitial stroma.[73] The complexity of the BM structure enables permeation and diffusion of selective molecules which impart filtration properties including the glomerular kidney BM responsible to filter blood.[74] Interaction of heparan binding growth factors including fibroblast growth factor (FGF), vascular endothelial growth factor (VEGF), and platelet-derived growth factor (PDGF) are achieved via perlecan and its heparan sulfate chain in the BM.[75–77] Storage and release of specific growth factors, ions, and hormones highlight its involvement in tissue development and remodeling processes.[78–83] For example, sequestered VEGF bound to heparan sulfate (perlecan) in the BM is involved in the development of new vasculature during an injury.[84–86] Moreover, apart from the provision of cell adhesion sites, the interaction of cell receptors to varying configurations of ligands on the underlying BM surface triggers a cascade of intracellular

reactions responsible for the altered behavior of cells in specific organs.[87,88] In addition to these biochemical cues, cell response is also controlled by biophysical cues such as BM architecture and elastic modulus,[89–91] Table 2. Substrate topography and mechanical properties modulate cell morphology, proliferation, migration, genetic expression, and activation of intracellular signaling pathways.[92–95] A wide variety of research involved in the field of mechanotransduction reveals the importance of understanding the structural properties of the BM.[96,97] Modulus measurement using AFM (atomic force microscopy), micro and nanoindentation have enabled researchers to investigate the young's modulus of various BM at different tissue locations.[98–100] Modulus measurements in the range of 1–3 MPa for chick inner limiting membrane and mouse retinal inner limiting membrane between 3.8 and 4.1 MPa has been reported.[4] However, Young's modulus is not universal and has varying values based on species age as well as tissue location.[101] Besides these mechanical BM properties, the structural features of BMs including thickness, porosity, and pore size significantly impact cellular behavior and function.[102–105] Transmission electron microscopy and scanning electron microscopy of the BM have revealed a fibrous structure with interconnected pores.[106–108] The undulated surface of the BM is characterized by fiber diameters in the range of 30–400 nm along with pores from 10–150 nm.[108–110] Due to its network structure, it also behaves like a physical barrier between the overlying cells and the underlying connective tissue, thereby controlling the movement of solutes and cells across it.[56,57] The arrangement of the BM structure is such that pores of an average size of 50 nm allow passive diffusion of small solutes.[52] Despite the small pore size, cells can transmigrate through the BM during an immune response or a normal tissue development event. Extensive studies in the literature have investigated cellular transmigration through the BM.[111–116]

In addition to the mentioned functions of the BM, its significance is further enhanced by the repercussion endured in the events of genetic abnormalities that lead to disorders such as Alport syndrome and Knoblach syndrome due to mutations in the type IV and XVIII collagen molecules, respectively.[117,118] These mutations affect the mechanical properties of the BM including the thickness and its stiffness. In the case of Alport syndrome, the collagen IV network is not highly cross-linked leading to a deformed pore and unstable thicker BM at the glomerular filtration barrier.[21] Mouse models representing Alport syndrome had a 30% lower Young's modulus compared with control mice despite a higher collagen IV content.[119] Similar thickening of vascular BM is observed during Alzheimer's disease due to the deposition of collagen IV and amyloid-β-accumulation.[120] Retinal vascular BM was observed to be thicker and softer in human patients with diabetes (1.5 kPa) compared with nondiabetic patients (5.1 kPa).[121] Moreover, an age-related increase in BM thickness has been supported by many studies.[15] Changes in biochemical

and biophysical properties of BM are observed during aging and disease progression as mentioned above, and their causes need to be investigated further.

In brief, the BM provides physical support and adhesion receptors to intermediate cells and a microenvironment rich in growth factors that influence cellular behavior such as proliferation, differentiation, and regenerative processes such as tissue repair. Research evidence also suggests the influence of structural and molecular diversity of the BM on cellular interactions, morphogenesis, and transmigration during immune surveillance as well as metastasis which further amplifies the need to incorporate such features in BM mimics.[122,123]

RECAPITULATING THE BM

Over the years, biomaterial research has produced an impressive amount of different synthetic material systems that can closely resemble a broad spectrum of essential native BM characteristics.[129] These BM mimics reach from simple porous polymeric membranes to highly structured electrospun fiber mats as well as 3D hydrogel systems (Figure 3) which can be produced from both natural and synthetic polymers or their arbitrary combinations. Considering their synthetic nature, engineered biomaterials can not only reduce the need for animal-derived products but also provide the opportunity to precisely tailor BM scaffolds to the biophysical and biochemical needs of a specific tissue region.[130,131] In this regard, a wide variety of macro- and microarchitectures could be realized based on different fabrication techniques, while advances in chemistry such as controlled peptide synthesis or click chemistry enable scaffold functionalization and adjustment of possible mechanical features.[132−137] These new synthetic BMs scaffolds not only replicate naturally derived BM but also are promising systems to improve on some of their limitations, including reproducibility and stable mechanical properties, and to study the effects of isolated BM properties on cellular behavior.

POROUS POLYMERIC MEMBRANES AS BM MIMICS

Biocompatible polymers such as poly(dimethylsiloxane) (PDMS), poly(carbonate) (PC), and poly(ethylene terephthalate) (PET) are widely used cell culture substrates. These polymer membranes are fabricated with pores via soft lithography (PDMS) or track etching (PET and PC) to enable the diffusion of nutrients and signaling molecules when used as support barriers across coculture models.[36,142] PDMS membranes have been employed as simple scaffolds to mimic the BM due to the ability to vary its elastic properties via manipulating the amount of cross-linker during its fabrication.[38,143−147] This allows for reducing the modulus of the membrane close to that of the BM.[148] Huh et al. developed a microfluidic device to mimic the alveolar-capillary barrier with the use of a 10 μm thick and porous PDMS membrane. This membrane was mechanically actuated to induce axial stretch of the PDMS and enabled an artificial breathing motion.[38] Similarly, the mechanical property of the PDMS membranes was further used by Stucki et al, where an array of alveolar coculture was actuated to stretch via passive perfusion of media through the channels of the chip.[149] Furthermore, to bring it closer to native BM dimensions, extremely thin PDMS membranes with 2 μm thickness have been fabricated with
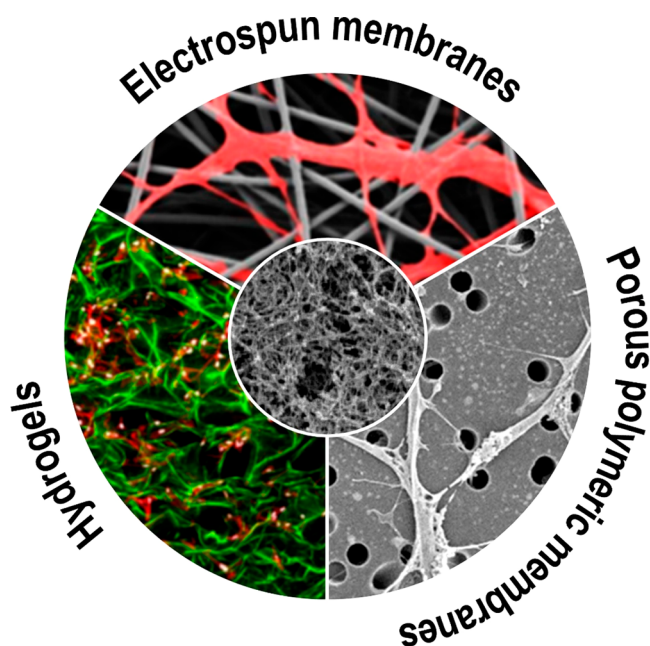

Figure 3. Structural resemblance of native basement membrane with synthetic mimics: Schematic represents the structural resemblances and differences observed by comparison of the scanning electron microscope (SEM) and confocal images between the Matrigel BM (center inset); adapted with permission from ref 138. Copyright 2006 Gelain et al. http://creativecommons.org/licenses/by/4.0/ (changes were made) and commonly used synthetic platforms including electrospun membranes (top); adapted with permission from ref 139. Copyright 2019 Ura, Daniel P et al. http://creativecommons.org/licenses/by/4.0/ (changes were made) and the hydrogels (bottom left); adapted with permission from ref 140. Copyright 2015 Elizabeth A. Wahl et al. https://creativecommons.org/licenses/by/3.0/ (changes were made) and track-etched membranes such as porous poly(ethylene terephthalate) (PET) (bottom right); adapted with permission from ref 141. Copyright 2018 Julian H. George et al. http://creativecommons.org/licenses/by/4.0/ (changes were made). Electrospinning allows alteration of membrane properties including thickness, fiber diameter, pore size, and fiber density, topography as well as mechanical properties. Synthesis of hydrogels with high water content also enables the formation of nonfibrous scaffolds with varying mechanical properties based on cross-linking density. However, despite the ease of handling and reproducibility, the use of porous polymeric membranes as synthetic BM mimics is controversial based on wide mechanical and topographical differences from the native BM.

controlled pore sizes of 3 and 5 μm to enable closer contact between astrocytes and endothelial cells to reconstruct relevant blood-brain barrier models.[150] Despite the ability to control thickness, pore size, and elastic modulus, PDMS is highly hydrophobic, which makes it difficult to support prolonged cell adhesion. Although surface treatments such as plasma and coating with ECM proteins have enabled their use in supporting cell layers,[151] these modifications are short-lived and do not allow long-term adhesion of sensitive primary cells.[151] Moreover, the hydrophobic nature of PDMS also leads to the adsorption of drugs and proteins from the media that can impact cell growth and physiology.[152] Other forms of porous polymers include PC and PET membranes that have been integrated into the popularly used Transwell inserts where they mimic BM to construct *in vitro* models for the blood-brain barrier, alveolar-capillary barrier (Figure 4), airway models, kidney glomerular, and skin tissue models.[153−160] The
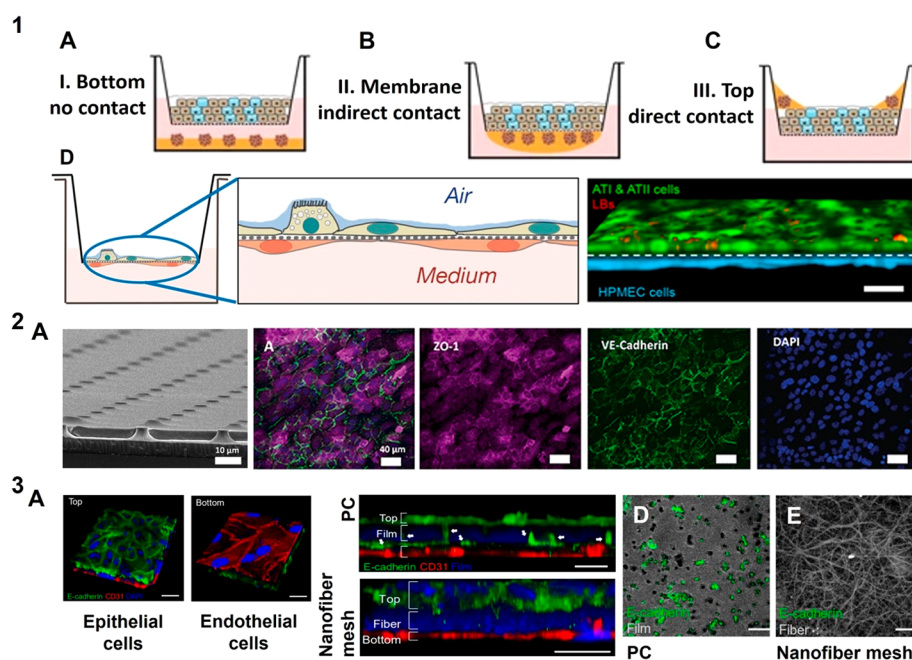
Figure 4. Porous polymeric membranes as basement membrane mimic: Depiction of possible combinations regarding cell coculture models using mechanically stable dense porous polymeric membranes: (1A) noncontact cocultures of two spatially separated cell types, (1B) indirect cocultures of two different cell types in contact with the same membrane, and (1C) direct mixture of two different cell types on top of the same membrane; adapted with permission from ref 164. Copyright 2017 Qiaozhi Lu et al. http://creativecommons.org/licenses/by/4.0/ (changes were made). (1D) Alveolar-capillary barrier models on permeable 0.4 μm pore size polyester membranes which can be introduced to an air−liquid interface represents the ease of handling coculture barriers on such mechanically robust platforms; adapted with permission from ref 165. Copyright 2021 Shinjini Chakraborty et al. http://creativecommons.org/licenses/by/4.0/ (changes were made). (2A) Mechanically tunable PDMS membranes and their reduced thickness to 2 μm were used to represent blood-brain barrier, by mono/coculture of endothelial cells and astrocytes where endothelial cells are stained for peripheral tight junctions ZO-1(red), adherens junction protein VE-cadherin (green); reprinted with permission from ref 144. Copyright 2020 Royal Society of Chemistry https://creativecommons.org/licenses/by/3.0/ (changes were made). Limitations of porous polymeric membranes are elucidated: (3A) Alveolar-capillary barrier on nanofiber PCL mesh and their cross-section on PC and nanofiber mesh which shows epithelial (green) transmigration toward the endothelial cells across a PC membrane (blue) with 3 μm pores compared to intact alveolar epithelial and endothelial cocultures on a nanofiber mesh, where the epithelial protrusion (green) is clearly seen on opposite side of (3D) PC membrane compared to the (3E) nanofiber mesh; reprinted with permission from ref 41. Copyright 2017 American Chemical Society (changes were made).

commercially available inserts are flexible in the choice of pore size and can be coated with ECM proteins to promote cell adhesion. However, they do not adequately represent the features of the BM as they lack interconnected porosity, fibrous architecture, and exhibit elastic modulus toward the higher end of the GPa range (Figure 3).[161] The group of Stone et al. has used such insert systems with 3 μm pore size to mimic the blood-brain barrier BM which supports four different cell types. In vitro, alveolar barrier models were also developed and optimized on transwell systems by Hermanns et al.[159] The group of Kasper et al. improved on these studies and conducted further research regarding the inflammatory and cytotoxic response of these alveolar-capillary models.[162] However, although basic BM features like the separation of cell monolayers or the study of basic disease models are possible, their mechanical and chemical properties are static and cannot be adapted to a specific in vivo BM microenvironment. The impact of the physical microenvironment on various cellular biological processes has been well established and highlights the importance of choosing the right scaffold to investigate in vitro organ models.[163] In our previous work, we showed a comparison of an alveolar-capillary model developed on a thin nanofibrous BM mimic with a conventional PET transwell insert membrane. It was found that the open network structure of the nanofiber mesh allowed a sufficiently direct contact and signal transfer between epithelial and endothelial

cells, while in PET membranes the epithelial cell penetrated through the pores and formed a rather imperfect cellular sheet at the endothelial side. However, the porosity of the PET membrane was significantly lower than that of the nanofiber mesh (14% vs 71%).[41] Another important observed feature was that 94% of CD31+ endothelial cells of the coculture models expressed α-SMA on PET compared with only 28% on the nanofiber membrane, and this was due to the difference in nanofiber topology and stiffness as compared with PET.[33] In another example, the significance of fibrous architecture on endothelial cell network forming capabilities has been justified further by Davidson et al.[41] They observed endothelial network formation on Matrigel and electrospun dextran methacrylate as long as cells were able to remodel and recruit the fibers on the respective scaffold. This describes the regulatory effect of mechanical features of an environment on various cellular activities. As a result, we can conclude that PC and PET polymer membranes might be obsolete in the recapitulation of specific organ BM functions. Despite the low production cost, ease of handling, and robust nature of the porous polymeric membranes, they are not entirely appropriate to replace and mimic the complex nature of the BM.

■ HYDROGEL AS BM MIMICS

Biocompatible hydrogels embellished with natural BM protein derivatives have been fabricated as a reminiscence of native
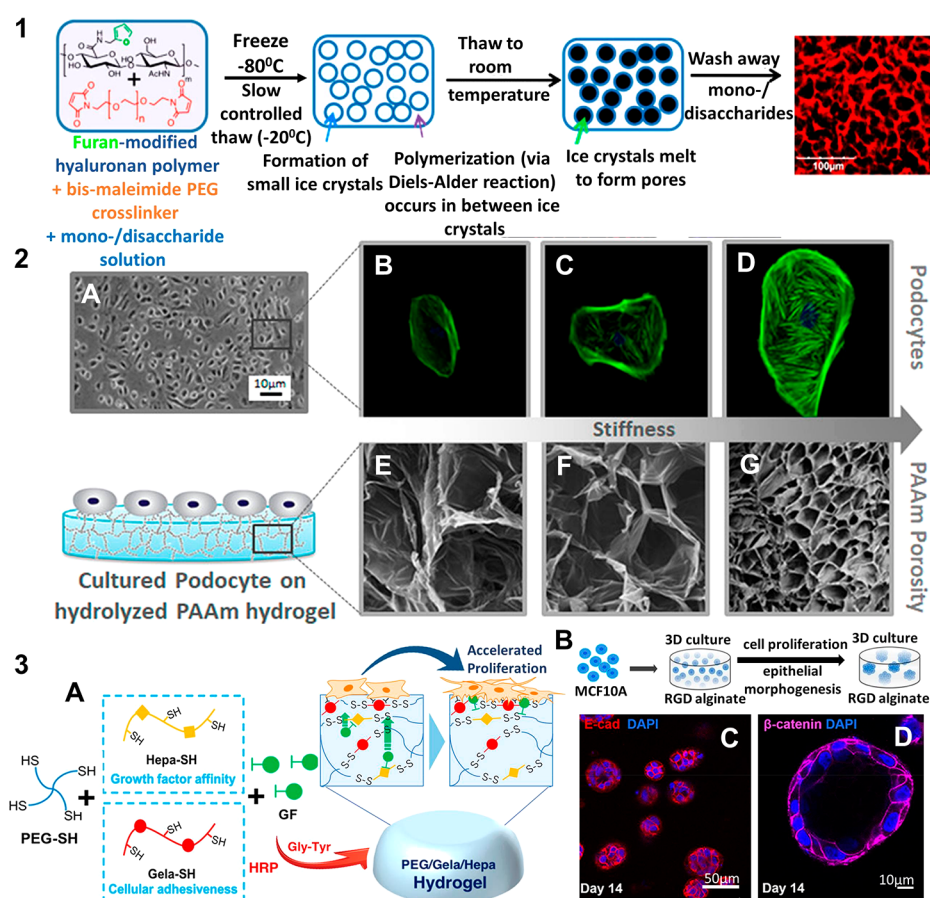
Figure 5. Optimization of hydrogel properties to mimic basement membrane structure and function: Modification of physical and chemical properties of hydrogels have been addressed in varying methods that allow their use as scaffolds to mimic BM: (1) Limitations of pore formation have been overcome using Diels−Alder click chemistry and cryo-gelation of the agarose and hyaluronic acid hydrogels. The polymer mixture is frozen, where the ice crystals slowly melt and are replaced by pores; reprinted with permission from ref 232. Copyright 2017 American Chemical Society; (2) Tunable physical properties of the hydrolyzed polyacrylamide (PAAm) such as stiffness (0.3−300 kPa) and pore size have been exploited to mimic the glomerular filtration barrier with the podocyte cells and also to study the influence of scaffold mechanical properties on such a filtration barrier *in vitro*; reprinted with permission from ref 248. Copyright 2019 American Chemical Society; (3A) Cell adhesion and proliferation on hydrogel BM mimics have been enhanced including the development of biofunctional PEG hydrogels using HRP mediated cross-linking of thiolated polymers, where the 4-arm PEG-SH was conjugated with thiolated gelatin (Gela-SH) and heparin (Hepa-SH); reprinted with permission from ref 249. Copyright 2019 American Chemical Society; (3B) hydrogels are commonly used to realize a 3D environment specifically for proliferation of breast epithelial cells as well as to mimic a tumor environment, where MCF10A cells are embedded in RGD functionalized alginate gels to form (3C) spheroids and (3D) acini like structures similar to *in vivo*; adapted with permission from ref 250. Copyright 2020 Barros de Silva. https://creativecommons.org/licenses/by/4.0/. Changes were made to copyright material.

BM.[166] Collagen I, laminin, fibrin, alginate, and hyaluronic acid have been used as components to fabricate cellular matrices or hydrogels that are close representatives of the BM environment.[39,167−169] Additionally, decellularized extracellular matrix (dECM) are emerging cell-free platforms that incorporate the native 3D tissue structure along with inherent bioactive features. These are derived from harvested organs and tissues that are made free of cells or extracted from long-term *in vitro* cell cultures.[170,171]

Some commonly used decellularized ECM-BM replicates commercially available are Matrigel (Corning), Geltrex (Invitrogen), and Cultrex (Trevigen). These are solubilized reconstituted BM extracts derived from Engelbrecht-Holm-Swarm (EHS) sarcoma mouse cells[172] and are widely used in maintaining organoids and human pluripotent stem cells. Geltrex has been used to maintain and scale up human pluripotent stem cells (hPSC) that can be used for downstream differentiation for therapeutic applications.[173] These naturally derived matrices have also been used to support and maintain various organoids including intestine, brain, inner ear, prostate, and lung.[174−178] However, although these matrices are of natural origin, there are limitations to their application as BM mimics such as precise working temperatures (4 °C) to prevent gelling, tuning their biochemical or biomechanical properties without influencing other material attributes,[166,179] and a lack of knowledge of their molecular composition. These factors tend to limit their translation.[180,181] However, the group of Mikhail et al. has used Matrigel together with collagen I to produce 3D hydrogels that support mini-gut culture. Collagen I provided mechanical support, and Matrigel offered key components of cell-adhesion present in BM, and when they were used in a perfusable microdevice, they offered support to intestinal stem cells for organoid formation.[182]

The organs from which dECM have been harvested range from skin,[183] lung,[184] cornea,[185,186] bladder,[186] kidney,[187] placenta,[188,189] amniotic membrane,[190−192] cartilage,[193] adipose tissue,[194,195] esophagus,[195] and liver[196] and have been used in organ regeneration and *in vitro* model construction.

Comercially available human decellularized dermal matrix (Glyaderm) was shown to enhance re-epithelialization and healed full thickness skin defects when seeded with adipose derived stem cells (ASC) in murine wound models.[197] Similarly, AlloDerm, provided structure and support to biologically engineered blood vessels which were mechanically stronger than vessels lacking AlloDerm ECM.[183] The group of da Mata Martins et al. demonstrated the importance of choosing appropriate decellularizing techniques to preserve the ultrastructures of decellularized human cornea where the epithelial BM (EBM) was preserved. This intact EBM structure was reported to differentiate the human embryonic stem cells to epithelial-like cells.[185] The influence of using native-like ECM scaffolds on cell proliferation and differentiation was supported by the work of Sobreiro-Almeida et al.[187] They fabricated a bioink based on unmodified porcine decellularised kidney ECM that supported the growth of renal progenitor cells which can be used to develop renal *in vitro* tissue models.[187] Another widely used biomaterial is decellularized placenta, which is rich in growth factors (fibroblast growth factor (FGF), platelet-derived growth factor (PDGF), vascular endothelial growth factor (VEGF), epidermal growth factor (EGF)),[198] ECM components,[199,200] and does not require invasive methods to isolate.[199] Human placenta-derived ECM was reported by Zhang et al. to induce and restore hair growing potential of highly passaged human papillary dermal cells.[201] Similarly, porous hybrid placental-ECM sponges (PIMS), derived by combining silk fibroin and placental ECM, displayed the potential to regenerate bone tissue.[202] Apart from placenta, decellularized amniotic membranes (the inner lining of the placenta) have also been exploited due to a rich pool of growth factors and intact BM component.[203] The group of Nasiry et al. reported the successful use of microporous 3D decellularised amniotic membranes scaffold for wound healing in diabetic rats.[204] Comparable to the native ultrastructural and molecular properties, the use of human amniotic membranes as scaffolds to support porcine urothelial cells was reported by group of Jerman et al.[205] Despite the ability to mimic the native tissue architecture and provision of bioactive cell adhesion sites and growth factors, the use of dECM is limited. These include undetected residual toxic substances post decellularization,[206] degradation rate of the scaffold,[207] batch to batch variability,[208] as well as undefined molecular composition.[209]

Another interesting biopolymer which has been widely used to mimic BM is silk fibroin. Silk fibroin is derived from *Bombyx mori* cocoons, and alone or in combination with other polymers, it has been used to produce mechanically stable, biofunctional, degradable, and biocompatible scaffolds.[210] Due to its versatile nature, silk fibroin has been widely used in tissue engineering including bone,[211] cartilage,[212] vascular,[213] and cancer models.[214] Stable silk fibroin by enzymatic cross-linking via horse radish peroxidase (HRP) have been employed as 3D mimics to study colorectal cancer cells.[215]

Comparatively, to some extent, synthetic hydrogels bear resemblance to the ECM, due to the presence of polymer networks formed via covalent and noncovalent interactions in the water-swollen environment.[216,217] Fine-tuning of their bulk mechanical properties by controlling the cross-linking and molecular density favors their use as BM mimics.[218,219] Frequently used polymers as hydrogels include polyacrylamide (PAAm), poly(ethylene glycol) (PEG), poly(acrylic acid) (PAA). Augmentation of hydrogels with peptides that represent ligands for cell attachment via integrins, protease degradative molecules, and a repertoire of growth factors bring it a step closer to its native counterpart.[220]

Biofunctionalization of hydrogels is achieved via the incorporation of short peptide sequences found in proteins such as collagen and laminin as seen in Figure 5.3. This enhances cellular binding via integrin to the hydrogel mimic.[221] A commonly used peptide sequence is RGD (Arg-Gly-Asp); however, IKVAV (Iso-Lys-Val-Ala-Val) and YIGSR (Tyr-Ile-Gly-Ser-Arg) are also used along with RGD to tune the cell adhesion property of the gel without affecting the mechanical property of the hydrogel.[222,223] Additionally, modified 3D silk fibroin hydrogels were covalently linked to IKVAV peptide via EDC/NHS, which promoted neural stem cell differentiation.[224]

To mimic vascular BMs, bioactivation of PEG hydrogels by RGD peptides of 20 and 10 kDa was achieved by the group of Gonzalez et al. The hydrogels featured a characteristic elastic modulus (84 and 55 kPa) and pore size (0.16 and 0.19 μm), which is similar to the natural vascular BM.[225] The influence of native characteristics and bioactivity was observed in favor of the hydrogels in terms of endothelial cell spread and expression of cellular adhesion molecules. On exposure to TNFα (Tumour necrosis factor), cells on hydrogels demonstrated an increased expression of VCAM (vascular cellular adhesion molecule) compared with that on control PC membranes, whereas E-selectin and ICAM (intercellular adhesion molecule) were not significantly different. Additionally, neutrophil capture on the hydrogels was 5 to 7-fold higher than that on stiff PC membranes. These results are similar to a 10-fold increase in neutrophil capture observed *in vivo* after LPS (Lipopolysaccharide) treatment. Furthermore, the study of bone and liver vascularization including the extent and maturity of vascular networks was conducted using 3D BM mimics by the group of Klotz et al.[226] They developed a hybrid of gelatin cross-linked with synthetic PEG hydrogels as vascular BM mimics. The cross-linking was achieved by factor XIII, where glutamine sequence was incorporated in 8-arm PEG that reacted with the lysine residue present in gelatin. This mimic was fabricated using unmodified cell binding ligands and also enables the incorporation of alternative bioactive compounds containing lysine residues.[226] Similarly, using the EDC/NHS reaction, cross-linking between PEG, collagen peptide (CLP), and RGD was achieved. The biofunctional cross-linked gels were used for neuronal cell cultures.[227]

Additionally, incorporation of matrix-metalloproteinases (MMPs)-cleavable peptides can impart degradable properties to the hydrogel. This is due to the degradative action of membrane-bound or cell-secreted enzymes, namely MMPs that are involved in ECM remodeling. Numerous cellular processes including proliferation and migration occur during the remodeling process to establish tissue homeostasis. The presence of MMP cleavable peptides in the hydrogels activates the degradation cascade of the BM mimic and also offers partial or complete replacement of the synthetic BM by cellular ECM deposits.[228,229] Incorporation of the peptide sequence recognized by membrane-type matrix metalloproteinase-1 (MT1-MMP) was achieved by the group of Ricardo et al.[230] The synthetic hydrogel was fabricated using four-armed maleimide-terminated PEG incorporated with cell adhesive peptides RGD as well as MT1-MMP degradable peptide sequences via Michael-type addition reaction. These function-

Table 3. Biomimetic Hydrogel Scaffolds Reproduced via Decellularized ECM, Synthetic or Natural Polymers to Replicate Tissue Microenvironments. The Table Describes the Synthesis of Hydrogels Using Different Chemical Approaches[a]

polymer	preparation method	pore size [μm], scaffold thickness [μm]	biofunctional component	cell line	tissue model	application	ref
gelatin 14%\HA tyramine 1% w/v	spin coating	-, 15.5 μm	KGF, FGF	Calu-3, A549, human MSC	respiratory epithelium	ECM mimic for MSC-derived epithelial patches	251
chitosan\dextran	Michael addition reaction	5–20 μm, -	FGF	NIH3T3	-	ECM mimics for wound healing	252
PEG-8SH\TEDVE	thioester exchange	-, -	GRGDS	human MSC	-	ECM mimics for MSC	253
GelMA	photoinitiated polymerization	-, 1000–2000 μm	-	human articular chondrocytes, human ECFC, human MSC, human OV-MZ-6	cancer models	3D ECM mimics	254
PEG diacrylate	-	-, 150 μm	collagen IV	human RPTEC, NHLF	acute kidney injury model	ECM mimics for renal epithelial cells	255
BPAA\diphenylalanine	π–π stacking	-, -	-	L929	-	ECM mimic	256
PNIPAM	radical polymerization	-, -	-	3T3-L1, HEK293, A549	-	ECM mimic	257
collagen\alginate\fibrin	hydrogen bond formation	40–120 μm, -	-	L929, MIN6, Y201 hMSC	musculoskeletal, pancreatic models	ECM mimic for soft tissues	258
collagen\laminin\HA	hydrogen bond formation	-, -	-	ratNPC	spinal cord injury	ECM mimic for neural tissue engineering	259
pLysAAm\HA	photopolymerization	150 μm, -	-	MCF-7	breast tumor	mimic breast tumor microenvironment	260
tetrazine and norbornene modified gelatin	biorthogonal cross-linking	-, -	-	hDPSC	3D hydrogels	compartmentalized cocultures	238
PEG	EDC/NHS	-, 500 μm	collagen peptide, RGD	rat neuron, rat astrocytes	cerebellar cell cultures	functional organoids	227
gelatin, alginate	Michael addition reaction, ionic reaction	400 μm, -	-	hMSC	-	adipose tissue engineering	261

[a]Keratinocyte growth factor (KGF), fibroblast growth factor (FGF), hyaluronic acid (HA), mesenchymal stem cells (MSC), eight arm-poly(ethylene glycol) (PEG-8SH), thioester di(vinyl ether) (TEDVE), gelatin methacryloyl (GelMA), 4-biphenylacetic acid (BPAA), poly-N-isopropylacrylamide (PNIPAM), collagen alginate and fibrin (CAF), poly-N-acryloyl L-lysine (pLysAAm), human lung adenocarcinoma cell line (Calu-3), human lung carcinoma epithelial cells (A549), mesenchymal stem cells (MSC), endothelial colony forming cells (ECFC), ovarian cancer cell (OV-MZ-6), renal proximal tubular epithelial cells (RPTEC), normal human lung fibroblast (NHLF), mouse fibroblasts (L929), mouse preadipocyte cells (3T3-L1), human embryonic kidney cells (HEK293), mouse pancreatic β cells (MIN-6), human TERT mesenchymal stem cells (Y201 hMSC), neural progenitor cells (NPC), human breast cancer cell line (MCF-7), human dental pulp stem cells (hDPSC).

alized and cross-linked hydrogels provided an optimal microenvironment and were reported to initiate renal epithelial tubulogenesis of the inner medullary collecting duct cells.[230] Such existing synthetic functionalized BM hydrogels with MMP-cleavable sequences provide platforms that can be used to understand and study remodeling processes involved in tissue repair, immune cell migration, and cancer metastasis. Moreover, controlled degradation alters the mechanical properties of the hydrogel which can further be exploited to activate cellular processes affected by substrate rigidity such as stem cell differentiation.[231]

Another aspect is the ability to artificially enrich the synthetic hydrogels with growth factors that regulate the wide array of cellular interaction and behavior analogous to the native BM microenvironment.[220] This is observed in hybrid agarose-hyaluronic acid hydrogels that allowed controlled spatial and gradient immobilization of biomolecules using photosensitive molecules via Diels−Alder click chemistry, which was developed by the group of Tam et al.[232] Two-photon irradiation exposed reactive sites to biomolecules present in the hydrogels and allowed investigation of endothelial cells exposed to a concentration gradient of modified vascular endothelial growth factor (VEGF-165). Additionally, these BM mimics allowed the embedding of MMP-cleavable peptides in the 3D hydrogel system offering the possibility to analyze metastatic migration through the hydrogels.

Cell-laden 3D hydrogels can be used to mimic complex tissue structures using printing techniques such as micro-extrusion, laser-assisted, inkjet, and stereolithography.[233,234] The group of Puperi et al. developed 3D PEG hydrogel based systems to recapitulate endothelialized aortic valve models by maintaining a coculture of vascular interstitial cells (VIC) and vascular endothelial cells (VEC).[235] Spatially controlled introduction of cell type-specific ligands in PEG hydrogels enabled the distribution of endothelial cells to the periphery and interstitial cells to the center, which is similar to the physiological distribution of cells in heart valves. This study could demonstrate that anisotropic cell type-specific ligand distribution can be used to control cell position in 3D matrices in order to study healthy and diseased conditions in vitro including cell metastasis, atherosclerosis, and drug response. To overcome shear stresses induced on cells during extrusion printing, a new method of digital light processing (DLP), which uses photopolymerization to print layer by layer 3D structures using cell embedded hydrogels. A 3D hydrogel combining silk fibroin and polyethylene glycol acrylate (PEG4A) was reported to maintain and proliferate human primary keratinocytes at an air−liquid interface.[236] Similarly, silk fibroin and glycidal methacrylate bioink developed by the groups of Kim et al. was used in DLP to produce precise scaffolds that can mimic tissues including heart, vessel, brain trachea, and ear.[237]

The benefits of using synthetic hydrogels were further justified by the ability to manipulate mechanical properties compared with conventional collagen gels to study various aspects of valve disease conditions.[235] The group of Contessi Negrini et al. established mechanically tunable 3D gelatin hydrogels modified using tetrazine and norbornene via biorthogonal click chemistry. By tuning the ratio of tetrazine to norbornene and their degree of modification, hydrogels ranging from 1 to 5 kPa were achieved that were used to embed human dental pulp stem cells.[238]

Moreover, the ability to manipulate shapes of synthetic PEG-diacrylate (PEGDA) hydrogels to mimic curved environments for ducts and acini of mammary glands presents the versatility and high level of control achievable with synthetic materials in the field of biomimetics. The curvature was achieved by using different molecular weight bilayers of PEGDA that swelled at different ratios by releasing from the underlying substrate. This together in combination with photopatterning provides another opportunity in the production of varying structures of ducts and acini, while additional cross-linking of PEGDA with gelatin methacrylate increases cell adherence to the substrate.[239] Freedom to manipulate hydrogel shape allows close resemblance to physiological structures that influences cell response and behavior in vitro.

Although the use of synthetic hydrogels offers the possibility to tune a broad spectrum of material properties such as stiffness, porosity, shape, and the spatially controlled incorporation of adhesive ligands and degradable sequences, hydrogel BM mimics still lack certain key characteristics found in native BMs. For example, the minimal achievable free-standing hydrogel thickness lies to date between 10 and 13 μm, which is at least 10 times thicker than native BMs.[225,240] This difference in scaffold thickness combined with the soft nature of hydrogels renders meaningful cocultivation of different cell types on opposing scaffold sides extremely challenging.[42,240−242] While the separation distance between cell layers is far too large for direct cellular communication, the softness of the material prevents cell cultivation on opposite sides of free-standing hydrogel layers.[242] However, these limitations can be overcome using support structures such as meshes and cross-linking chemistry to improve hydrogel stability.[240,243,244] The group of Zamprogno et al. was successful in establishing an alveolar-capillary coculture model on a ∼10 μm thick collagen-elastin supported on a gold mesh.[240] 3D gelatin methacrylolyl (GelMA) hydrogel scaffolds were designed to mimic lung alveoli structures to support alveolar cells on a less than 3 mm thick hydrogel at air−liquid interface.[243] Despite thickness limitations and lack of fibrous structure, hydrogels are popularly used to mimic the intricate 3D microenvironment of tissues using printing approaches and photopatterning of cell-laden gels.[245,246] Successful 3D structures in microfluidic chips have been achieved by photopatterning of cell-laden gelatin hydrogels (Table 3).[247]

◼ ELECTROSPUN BM MIMICS

Electrospinning is a versatile technique that enables the production of micro to nanofibrous scaffolds that can be modulated in terms of their surface morphology, fiber diameter size, mesh thickness, and fiber arrangement.[262] Multiple synthetic polymers ranging from poly(caprolactone) (PCL), poly(lactic acid) (PLA), poly(glycolic acid) (PGA), poly-(lactic-co-glycolic acid) (PLGA), as well as polymers of natural origin including chitin, collagen, gelatin, and their hybrids have been utilized to produce diverse electrospun scaffolds in the field of tissue engineering.[263]

The potential of achieving desired mechanical (pore size, fiber diameter, topology) and chemical (functionalization) properties by varying electrospinning parameters, including polymer, solvent, flow rate, distance, voltage supply, and so on, has been exploited to tailor BM mimics. Many such in vitro models include tissue models of skin, glomerular filtration units as well as alveolar-capillary barrier models.[43−48] A natural polymer, laminin I, extracted from murine has been electro-
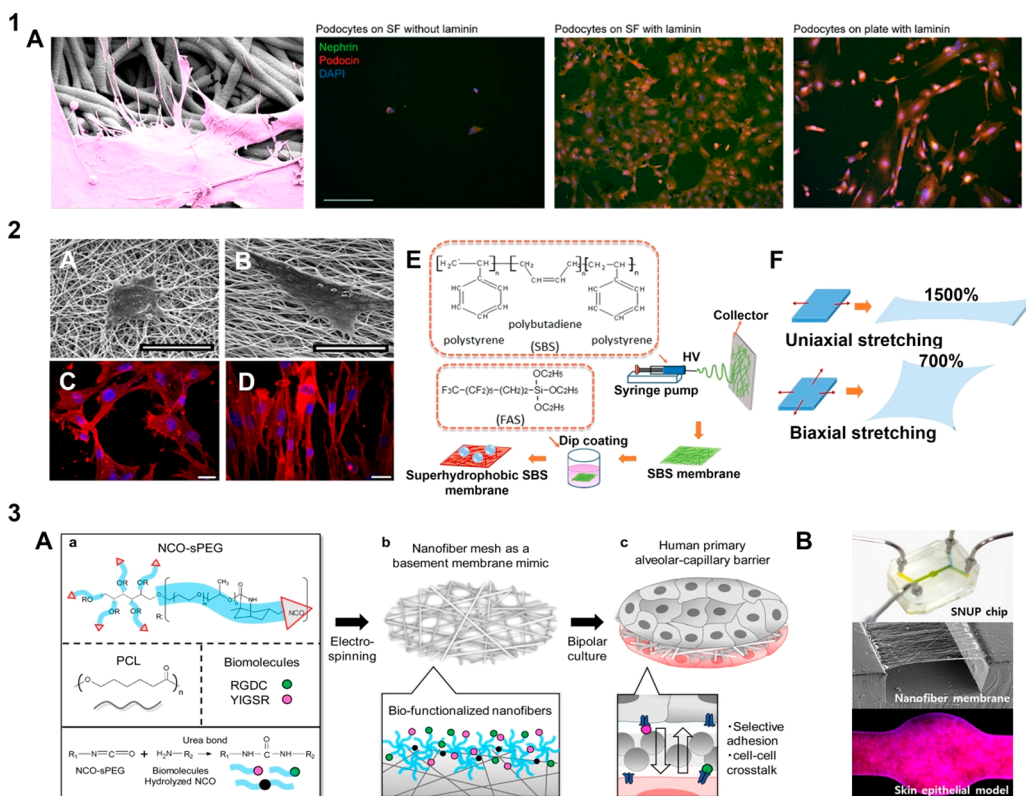
Figure 6. Fibrous basement membrane mimics: Electrospinning is a versatile technique to produce fibrous scaffolds of varying properties in order to mimic the native BM in terms of architecture strength and dimensions of the fibers: (1A) A laminin-coated nanofibrous membrane of silk fibroin (SF) was fabricated as glomerular BM mimic, for differentiation of human podocytes from human stem cells, where (A) a podocyte interacts with the laminin coated SF fibers and confocal images of podocytes stained for podocin (red), nephrin (green) and nucleus (blue), on SF without laminin, SF with laminin and on tissue culture plate; adapted with permission from ref 277. Copyright 2022 Mou, Xingrui et al. https://creativecommons.org/licenses/by/4.0/ (changes were made). (2) Varying mechanical and topographical properties is possible where (A−D) random and aligned forms of PCL-gelatin meshes are exploited to mimic specific BM, where NIH3T3 cells are shown to respond respectively by cellular spread or elongation; adapted with permission from ref 295. Copyright 2016 Fee et al. https://creativecommons.org/licenses/by/4.0/ (changes were made). (E,F) optimization of elastic modulus can be achieved where superhydrophobic and elastic fibers were fabricated by dip coating poly(styrene−butadiene-styrene) (PBS) fibers in fluoroalkyl silane (FAS) to produce fibers that can be stretched both uniaxially (1500%) and biaxially (700%) even after 1000 stretch cycles; adapted with permission from ref 296. Copyright 2015 Hua Zhou et al. http://creativecommons.org/licenses/by/4.0/ (changes were made). (3) Electrospinning allows biofunctionalization as seen in (A) synthetic alveolar-capillary BM for *in vitro* expansion and study of pulmonary cells, where electrospinning of PCL and the surface segregated isocynate end groups of six-armed sPEG form covalent bonds with the amine groups of bioactive peptides via urea bond formation; reprinted with permission from ref 41. Copyright 2017 American Chemical Society (no changes); (B) Electrospun fibers can also be used as free-standing membranes in microfluidic chips to analyze effect of dynamic shear on cells; reprinted with permission from ref 297. Copyright 2021 American Chemical Society (changes were made).

spun to produce nanofibrous scaffolds that mimic BM in aspects of morphology including fiber diameter, pore size as well as architecture. Unlike electrospun biopolymers including collagen and fibronectin, laminin does not require cross-linking modification steps to maintain its fibrous morphology when exposed to an aqueous environment.[264,265] The group of Neal et al. fabricated electrospun laminin I nanofibers without cross-linking modification. The scaffold maintained a fibrous morphology even after exposure to cell culture media.[266] This property was attributed to the use of lyophilized laminin, which is considered to be insoluble in aqueous media and also to possible structural changes in the protein during elctrospinning that make the laminin insoluble in an aqueous media.[267,268] However, use of laminin nanofibers as an alternative platform to mimic BM is still limited. Since commercially available laminin is majorly derived from human placenta and exhibit batch-to-batch variability. Moreover, compared to other ECM proteins, laminin is expensive due to difficulties in obtaining sufficient yields of its active

form. Thus, it is mainly used to culture specialized cells like neuronal stem cells.[269]

Silk fibroin, alone or in combination with other natural polymers has been used to produce mechanically stable and biocompatible nanofibrous scaffolds.[270,271] Electrospun silk fibroin has been used successfully to support many tissue cells including cartilage,[272] mucosal cells,[273] bone,[274] endothelial,[275] and nerve cells.[276] Electrospun silk fibroin nanofibers fabricated by Mou et al. (Figure 6.1) were successfully used to mimic glomerular BM, which supported the proliferation and differentiation of human podocytes.[277] Additionally, a hybrid silk fibroin and chitin nanofibers were incorporated with TGF-β, to support the adhesion and proliferation of chondrocytes.[278] Apart from bone tissues, electrospun silk fibroin has also been used to produce stable vascular grafts that proliferate endothelial cell growth.[279] In addition, laminin-coated electrospun silk fibroin mats have been promising tools for proliferation and differentiation of neural progenitor cells.[280] Moreover, a combination of electrospinning and

microfluidics has been used to produce layer by layer pure silk nanofibers and their microdroplets to sustain endothelial cell monolayers and prevent thrombus formation.[281]

The use of hybrid blends of both natural and synthetic polymers to fabricate a scaffold has been frequently considered. For example, decellularized kidney ECM from porcine and PCL blend was electrospun to fabricate kidney filtration BM mimic by Sobreiro-Almeida et al.[282] They concluded that the high content of ECM in the polymer blend aided in closer representation of the renal BM and enhanced cell line biological activity such as adhesion, proliferation, and migration as well as the formation of tight junctions compared to pure synthetic PCL scaffolds. Another group of Slater and colleagues have also successfully developed a trilayer glomerular filtration model that includes an electrospun layer of collagen I and PCL blend that is physically supported on a micro photoelectroformed (PEF) nickel mesh to recapitulate the glomerular BM. This artificial BM is fixed onto a cell crown followed by coculture of immortalized cell lines of GEnC (glomerular endothelial cells) and podocytes on opposite sides of it. They were able to demonstrate a monolayer formation of GEnC and a semimonolayer formation of the podocyte cell layers on the opposite sides of the BM mimic.[34]

Moreover, the potential of electrospun fibers to maintain cell growth and prevent cell infiltration was proposed by the group of Bye et.al. They recapitulated skin BM by fabrication of a triple-layered electrospun scaffold composed of nanoporous poly hydroxybutyrate-co-hydroxyvalerate nanofibers sandwiched between two layers of microporous poly L-lactic acid microfibers. This 3D scaffold not only allowed adherence and proliferation of keratinocytes and fibroblast cell layers on the opposite sides but also impeded cell infiltration. Despite the physical impedance to the movement of cells, the formation of a developed epithelium indicates the ability of keratinocytes and fibroblast cell layers to communicate with each other across the BM mimic.[283]

Scaffolds comprised of pure synthetic polymers have also been adapted to support cell adhesion and proliferation. Electrospinning permits conjugation of cell adhesive sequences to obtain biofunctionalized scaffolds that enable efficient and long-term adhesion of primary cells in particular.[262,284] The group of Mollet et al. established a synthetic BM mimic by electrospinning ureidopyrimidinone (UPy)-PCL polymers and functionalized it with UPy-peptides. The hierarchical arrangement of the fibrous micro and nanofibers of UPy-PCL along with the presence of a customized bioreactor accentuated its likeness to the naturally occurring BM environment of the renal tubule epithelial cells. Human kidney 2 (HK2) cells were observed to proliferate on the freestanding mimics under both static and dynamic conditions maintained in customized bioreactors that allowed separate media flow on the apical and basal side of the cells.[40]

Furthermore, evidence of the use of biofunctionalized electrospun fibers as biomimetic BM in the establishment of a bipolar coculture model of alveolar-capillary barrier (Figure 6.3) is observed in the works of Nishiguchi et al. A 10 μm thick mesh was fabricated via electrospinning of PCL and bioinert six-armed, star-shaped poly(ethylene oxide-stat-propylene oxide) with isocyanate end groups (NCO-sPEG) and functionalized via short RGD peptide sequences. Resembling the BM of the alveolar-capillary barrier, the electrospun mimic provided a scaffold where human primary pulmonary alveolar epithelial cells (HPAEC) and human umbilical vein

endothelial cells (HUVEC) were successfully proliferated as monolayers on opposite sides as a bipolar culture. This work also portrayed the eccentric behavior of the HPAEC infiltration to the HUVEC layer when seeded on PC membranes of commercially available transwell inserts.[41]

Apart from obtaining biofunctionalized scaffolds as an important criteria for cell adhesion, the cells often respond to the mechanical and topographical features of substrates as well. The significance of scaffold thickness, porosity, and fibrous architecture on the formation of the functional alveolar-capillary barrier was highlighted by Jain et.al. by comparing ultrathin 2 μm electrospun nonwoven PCL meshes with commercial 10 μm thick PET membranes.[33] The 21 days' stable coculture model demonstrated integral barrier formation and the absence of cell layer infiltration despite the highly porous and ultrathin nature of the PCL meshes. Interestingly, these models displayed a similar response as in vivo when induced with inflammation using IL8 where the neutrophils transmigrated across the double cell layers and the BM mimic to reach the site of cytokine addition. This highlights that universally required porous polymeric membranes with 3 μm pores or large can be replaced by electrospun fibers for such investigations (Figure 4.3). Besides demonstrating successful neutrophil migration, the endothelial cells expressed a higher percentage of mesenchymal marker αSMA (smooth muscle actin) on PET membranes compared with that on PCL meshes, which further supports the influence of scaffold on cell behavior.

Moreover, electrospinning of synthetic polymers also allows the incorporation of bioactive molecules including MMP-cleavable sequences to fabricate BM mimics with controllable mechanical and physical properties. Kim et al. fabricated nanofibers that released DNA linked to the fibers by MMP cleavable sequence in response to high MMP presence during diabetic ulcers.[285] This was achieved by using a PCL−PEG block copolymer that had surface-exposed amine groups. The MMP cleavable sequence was linked to the fiber via amine groups and the linear polyethelineimine (PEI) was chemically conjugated to the MMP sequence. Due to electrostatic interaction, the DNA molecules bound to the linear PEI and DNA release were confirmed in the presence of MMP. Despite the ability to chemically modify, these synthetic mimics lack water retention and flexibility to an extent compared with the natural ECM and hydrogels. This limitation was addressed by electrospinning of methacrylated hyaluronic acid along with a photoinitiator and carrier polymer to produce photo-cross-linkable fibrous hydrogels.[286] Similarly, electro-conductive nanofibers were fabricated using a blend of gelatin-polyaniline, and a blend of hydrogel gelatin and 4-armed PEG, using novel cross-linking chemistry, to mimic retinal BM.[287]

Furthermore, improvements by incorporation of protease-sensitive motifs in electrospun hyaluronic acid were carried out by Wade et al.[288] Michael addition reaction between maleimides and thiols was exploited by using hyaluronic acid modified with maleimide and methacrylated cleavable peptides. Moreover, other cell adhesive peptides can also be embedded in these fibrous scaffolds. This allows the production of electrospun hydrogels that closely resemble the native BM with respect to fibrous architecture as well as the presence of bioactive molecules that play a major role in cell behavior and response.

Although synthetic electrospun scaffolds are ideal platforms to mimic BM, they are unable to completely resemble the 3D

Table 4. Biomimetic Scaffolds Reproduced via Electrospinning Using Natural, Synthetic Polymers, or a Combination of Both in Various Fields of Tissue Engineering to Obtain Close Representatives of the BM. The Table Describes Various Electrospun Mimics with Their Characteristic Parameters and Morphological Properties along with Biofunctional Components[a]

polymer	solvent	spinning properties flow rate [mL/h], collecting distance [cm], voltage [kV]	fiber diameter [nm], porosity [%], scaffold thickness [μm]	biofunctional component	cell line	tissue model	application	ref
laminin I	HFIP	1.5 mL/h, 12.5 cm, 20 kV	142 nm, -, -	-	hASC	-	BM mimic for neural tissue engineering	298
PCL	HFIP	0.5 mL/h, 15 cm, 18 kV	400 nm, -, -	porcine dKECM	HK-2	-	renal filtration barrier	282
PET	TFA	1 mL/h, 15 cm, 15 kV	200–600 nm, 83%, 35 μm	gelatin	hEC	vascular graft	blood vessel tissue engineering	299
PCL\SF	HFIP	0.2–1.5 mL/h, 8.5 cm, 20 kV	146 nm, -, -	porcine BM extracts	primary epithelial cell	-	esophageal tissue engineering	300
PLGA	acetone	0.5 mL/h, 16 cm, 13 kV	300 nm, -, 20 μm	peptides derived from fibronectin, laminin, collagen IV	HF, HaCaT,	skin model	BM mimics for long-term cell coculture.	301
SF\PEO	water	1.2 mL/h, 14 cm, 12 kV	267 nm, 54%, -	laminin	ratSC	-	peripheral nerve tissue engineering	302
PCL	MC:DMF (80:20)	1 mL/h, 12 cm, 13 kV	135–1095 nm, -, -	Matrigel	C17.2	-	nerve tissue engineering	303
PLLA	CF:DMF (4:1 v/v)	0.2 mL/h, 18 cm, 22 kV	1380 nm, 52%, 100 μm	ASA, AM lysate	HUVEC	-	endothelial BM	304
PLGA	HFIP	0.36 mL/h, 15 cm, 14 kV	308 nm, -, -	elastin	SIMS	-	salivary gland BM	305
4%PEG, 96%PCL	TFE	1 mL/h, 10 cm, 10 kV	500 nm, -, 6 μm	collagen I	TIME, human astrocyte, human pericyte	-	blood brain barrier	306
PCL	HFIP	0.35 mL/h, 15 cm, 21 kV	260 nm-350 nm,-,2 μm	collagen I, fibronectin, laminin	HPMEC, NCI-H441	-	alveolar-capillary barrier	33
PCL	HFIP	0.5 mL/h, 15 cm, 20 kV	300 nm, -, 10 μm	peptides derived from fibronectin	HUVEC, HPMEC, NCI-H441, HPAEC	-	alveolar-capillary barrier	41
PCL	HFIP	1.2 mL/h, 12 cm, 18.5 kV	220–340 nm, -, -	ureido pyrimidinone peptide functionalized	HK-2	-	kidney glomerular filtration barrier	40
gelatin-polyaniline and gelatin 4-arm PEG	acetic acid water, NMP	1.5 mL/h, 9 cm, 23 kV	154 nm, -, 4000 μm	-	hRPE	retinal Bruchs membrane	age-related macular degeneration	287

[a]1,1,1,3,3,3-hexaflouro-2-propanol (HFIP), decellularized kidney extracellular matrix (dKECM), poly-L-lactic acid (PLLA), acetylsalicylic acid (ASA), amniotic membrane (AM),poly lactic-co-glycolic acid (PLGA), 2,2,2-trifluoroethanol (TFE), poly ethyleneglycol (PEG), poly(ε-caprolactone) (PCL), N-methyl-2-pyrrolidone (NMP), human adipose stem cells (hASC), human kidney cell line (HK-2), human coronary artery endothelial cells (hEC), human dermal fibroblast (HF), human keratinocyte cell line (HaCaT), SC (Schwann cells), neonatal mouse cerebellum stem cells (C17.2), human umbilical vein endothelial cells (HUVEC), mouse ductal submandibular epithelial cells (SIMS), telomerase immortalized microvascular endothelial cells (TIME), human pulmonary microvascular endothelial cells (HPMEC), human lung adenocarcinoma epithelial cell lines (NCI-H441, human primary pulmonary alveolar epithelial cells (HPAEC), human kidney cell lines (HK-2), human retinal pigmented epithelium (hRPE).

complexity of the natural form which is responsible for regulating various cellular functions.[56,289] Electrospinning can be combined with other techniques including the manual folding and unfolding of nanofiber mesh where 3D electrospun nanofibers can be achieved by stacking layers of cell laden nanofibers or centrifugal electrospinning.[290,291] However, these techniques are limited due to operator skill as well as limited fiber morphology using centrifugal electrospinning. The mechanical stability offered by fibrous electrospun scaffolds allows their use as freestanding substrates for 2.5D cocultures on opposite sides of the BM mimic seen in alveolar-capillary barrier models supported on electrospun biofunctionalized PCL membranes[41,292] and in microfluidic devices that represent *in vitro* glomerular filtration models.[40] However, electrospinning is limited in terms of reproducibility due to high dependence on environmental factors such as humidity and temperature.[293] The choice of solvents and high voltage used during electrospinning can also lead to loss of bioactivity of biomolecules (Table 4).[294]

CONCLUSION AND FUTURE PERSPECTIVES

BM is a vital form of ECM that offers physical support; divides tissues into distinct regions; and provides cues for cellular differentiation, proliferation, and transmigration. The unique structure and composition of the BM at different anatomical locations necessitates the fabrication of mimics that can be tailored to accurately represent specific organ models.[55,56] However, the use of naturally derived materials as BM mimics is challenging considering their lot-to-lot variability and difficulty in amending their respective biophysical and biochemical properties.[166,179]

Porous and nonporous polymeric membranes have been widely used to replace natural BM in *in vitro* models due to the ease of handling and mechanical robustness (Figure 4). Although these membranes display some key features such as nano- or microporosity, their simplicity in terms of topography and biochemical cues are far from representing the native BM.

Another major synthetic substitute for mimicking the BM are hydrogels. These scaffolds are highly modifiable and allow the adjustment of nanoporosity as well as bulk mechanical properties by cross-linking processes. Additionally, bioactive compounds can be incorporated into the hydrogel, which enables cellular remodeling and provides vital biochemical cues such as adhesive motifs or the spatiotemporal release of growth factors. Despite their lack of fibrous architecture, cell-laden hydrogels aided by 3D printing techniques have been employed to mimic and construct complex tissue microenvironments.[234]

Additionally, electrospinning has been widely and successfully used in the development of synthetic and hybrid BM, which due to their mechanical stability, indirectly support cocultures while accurately incorporating the dimensions of natural BM.[34,40,41,283,301,307] The versatility of electrospinning with regard to the source material and the collection method enables the optimization of topographical, biomechanical, and biochemical scaffold properties of the ultimate product.[41,262] As a result, electrospun membranes can be tailored precisely to a specific BM region, while offering additional perks such as defined fiber diameter, topographical guidance, adhesive and degradable motifs.[284] Moreover, the fabrication of scaffolds from stimuli-responsive polymers can provide additional benefits exceeding the capabilities of natural BM, where

cellular actuation is induced by external stimuli including pH, temperature, electrical current and light.[308]

The importance of the choice of scaffold depends on the extent of physical and chemical stability required to mimic the respective organ or tissue system, resources available as well as cellular responses.[32−34] It is critical to elucidate native cell−BM interaction and improve the fabrication of *in vitro* models as reliable constructs in regenerative medicine. Stable scaffolds for such reproducible *in vitro* models can be achieved by combining the tunable physical and mechanical properties of synthetic polymers together with the biochemical cues of natural polymers.[309−311] Furthermore, dynamic gradients in stiffness can be created at the cell matrix interface to mimic BM in health and disease conditions.[312,313]

However, vital questions such as the extent of resemblance in terms of composition and mechanical, structural as well as topographical cues to mimic the BM are still unanswered. The BM is constantly evolving and unique at various organ locations in terms of architecture, composition, and functionality during both physiological and pathological events. There is an existential gap of knowledge that can be filled by implementing novel techniques such as computational modeling, imaging techniques, and gene sequencing. Advances in imaging techniques such as 4D imaging and noninvasive mechanical measurements including ultrasound, optical coherence tomography, and magnetic resonance elastography can be exploited to gain insights into the native BM.[212,314,315] Our understanding of answers to such predominant questions would enable the construction of scaffolds to maintain the stability and functionality of *in vitro* models. The inputs gained from these novel techniques can be integrated to develop simulated models of representative BM, which can further be used as guides to design scaffolds that can realize native properties in the *in vitro* models. This could open doorways to construct reliable mimics of BM tailored to support *in vitro* models in the field of tissue engineering and regenerative medicine.

AUTHOR INFORMATION

Corresponding Author

Smriti Singh − *Max-Planck-Institute for Medical Research, Heidelberg 69028, Germany;* orcid.org/0000-0002-2164-9912; Email: smriti.singh@mr.mpg.de

Authors

Puja Jain − *DWI-Leibniz-Institute for Interactive Materials e.V, Aachen 52074, Germany*
Sebastian Bernhard Rauer − *Chemical Process Engineering, RWTH Aachen University, Aachen 52074, Germany*
Martin Möller − *DWI-Leibniz-Institute for Interactive Materials e.V, Aachen 52074, Germany;* orcid.org/0000-0002-5955-4185

Complete contact information is available at:
https://pubs.acs.org/10.1021/acs.biomac.2c00402

Notes

■ REFERENCES

(1) Frantz, C.; Stewart, K. M.; Weaver, V. M. The extracellular matrix at a glance. *J. Cell Sci.* **2010**, *123* (24), 4195−4200.

(2) Stevens, M. M.; George, J. H. Exploring and engineering the cell surface interface. *Science* **2005**, *310* (5751), 1135−1138.

(3) Kefalides, N. A.; Borel, J. P. Morphology and ultrastructure of basement membranes. *Curr. Top. Membr.* **2005**, *56*, 19−42.

(4) Candiello, J.; Balasubramani, M.; Schreiber, E. M.; Cole, G. J.; Mayer, U.; Halfter, W.; Lin, H. Biomechanical properties of native basement membranes. *FEBS J.* **2007**, *274* (11), 2897−2908.

(5) Breitkreutz, D.; Koxholt, I.; Thiemann, K.; Nischt, R. Skin Basement Membrane: The Foundation of Epidermal Integrity—BM Functions and Diverse Roles of Bridging Molecules Nidogen and Perlecan. *BioMed. Res. Int.* **2013**, *2013*, 179784.

(6) Farhadian, F.; Contard, F.; Sabri, A.; Samuel, J.; Rappaport, L. Fibronectin and basement membrane in cardiovascular organogenesis and disease pathogenesis. *Cardiovasc. Res.* **1996**, *32* (3), 433−442.

(7) Miner, J. H. The glomerular basement membrane. *Exp. Cell Res.* **2012**, *318* (9), 973−978.

(8) Hahn, E.; Wick, G.; Pencev, D.; Timpl, R. Distribution of basement membrane proteins in normal and fibrotic human liver: collagen type IV, laminin, and fibronectin. *Gut* **1980**, *21* (1), 63−71.

(9) Pardridge, W. M. Blood-brain barrier biology and methodology. *J. Neurovirol.* **1999**, *5* (6), 556−569.

(10) Simon-Assmann, P.; Simo, P.; Bouziges, F.; Haffen, K.; Kedinger, M. Synthesis of basement membrane proteins in the small intestine. *Digestion* **2004**, *46* (Suppl. 2), 12−21.

(11) Torricelli, A. A.; Singh, V.; Santhiago, M. R.; Wilson, S. E. The corneal epithelial basement membrane: structure, function, and disease. *Invest. Ophthalmol. Vis. Sci.* **2013**, *54* (9), 6390−6400.

(12) West, J.; Mathieu-Costello, O. Structure, strength, failure, and remodeling of the pulmonary blood-gas barrier. *Annu. Rev. Physiol.* **1999**, *61* (1), 543−572.

(13) Worthley, D. L.; Giraud, A. S.; Wang, T. C. The extracellular matrix in digestive cancer. *Cancer Microenviron.* **2010**, *3* (1), 177−185.

(14) Xu, L.; Nirwane, A.; Yao, Y. Basement membrane and blood−brain barrier. *Stroke Vasc. Neurol.* **2019**, *4* (2), 78−82.

(15) Halfter, W.; Oertle, P.; Monnier, C. A.; Camenzind, L.; Reyes-Lua, M.; Hu, H.; Candiello, J.; Labilloy, A.; Balasubramani, M.; Henrich, P. B.; Plodinec, M. New concepts in basement membrane biology. *FEBS J.* **2015**, *282* (23), 4466−4479.

(16) Kruegel, J.; Miosge, N. Basement membrane components are key players in specialized extracellular matrices. *Cell. Mol. Life Sci.* **2010**, *67* (17), 2879−2895.

(17) Mak, K. M.; Mei, R. Basement membrane type IV collagen and laminin: an overview of their biology and value as fibrosis biomarkers of liver disease. *Anat. Rec.* **2017**, *300* (8), 1371−1390.

(18) Morrissey, M. A.; Sherwood, D. R. An active role for basement membrane assembly and modification in tissue sculpting. *J. Cell Sci.* **2015**, *128* (9), 1661−1668.

(19) Yang, H.; Borg, T. K.; Wang, Z.; Ma, Z.; Gao, B. Z. Role of the basement membrane in regulation of cardiac electrical properties. *Ann. Biomed. Eng.* **2014**, *42* (6), 1148−1157.

(20) Pozzi, A.; Yurchenco, P. D.; Iozzo, R. V. The nature and biology of basement membranes. *Matrix Biol.* **2017**, *57*, 1−11.

(21) Thorner, P. S. Alport syndrome and thin basement membrane nephropathy. *Nephron Clin. Pract.* **2007**, *106* (2), c82−c88.

(22) Naylor, R. W.; Watson, E.; Williamson, S.; Preston, R.; Davenport, J. B.; Thornton, N.; Lowe, M.; Williams, M.; Lennon, R. Basement membrane defects in CD151-associated glomerular disease. *Pediatr. Nephrol.* **2022**, *2022*, 1−11.

(23) Smyth, N.; Vatansever, H. S.; Murray, P.; Meyer, M.; Frie, C.; Paulsson, M.; Edgar, D. Absence of basement membranes after targeting the LAMC1 gene results in embryonic lethality due to

failure of endoderm differentiation. *J. Cell Biol.* **1999**, *144* (1), 151−160.

(24) Bruckner-Tuderman, L.; Has, C. Disorders of the cutaneous basement membrane zone—the paradigm of epidermolysis bullosa. *Matrix Biol.* **2014**, *33*, 29−34.

(25) Medeiros, C. S.; Marino, G. K.; Santhiago, M. R.; Wilson, S. E. The corneal basement membranes and stromal fibrosis. *Invest. Ophthalmol. Vis. Sci.* **2018**, *59* (10), 4044−4053.

(26) Ingangi, V.; Minopoli, M.; Ragone, C.; Motti, M. L.; Carriero, M. V. Role of microenvironment on the fate of disseminating cancer stem cells. *Front. Oncol.* **2019**, *9*, 82.

(27) Paul, C. D.; Shea, D. J.; Mahoney, M. R.; Chai, A.; Laney, V.; Hung, W.-C.; Konstantopoulos, K. Interplay of the physical microenvironment, contact guidance, and intracellular signaling in cell decision making. *FASEB J.* **2016**, *30* (6), 2161−2170.

(28) Stylianopoulos, T.; Munn, L. L.; Jain, R. K. Reengineering the physical microenvironment of tumors to improve drug delivery and efficacy: from mathematical modeling to bench to bedside. *Trends Cancer* **2018**, *4* (4), 292−319.

(29) Weinstein, N.; Mendoza, L.; Gitler, I.; Klapp, J. A network model to explore the effect of the micro-environment on endothelial cell behavior during angiogenesis. *Front. Physiol.* **2017**, *8*, 960.

(30) Zhu, L.; Luo, D.; Liu, Y. Effect of the nano/microscale structure of biomaterial scaffolds on bone regeneration. *Int. J. Oral Sci.* **2020**, *12* (1), 1−15.

(31) Li, J.; Liu, Y.; Zhang, Y.; Yao, B.; Li, Z.; Song, W.; Wang, Y.; Duan, X.; Yuan, X.; Fu, X. Biophysical and biochemical cues of biomaterials guide mesenchymal stem cell behaviors. *Front. Cell Dev. Biol.* **2021**, *9*, 397.

(32) Baker, B. M.; Trappmann, B.; Wang, W. Y.; Sakar, M. S.; Kim, I. L.; Shenoy, V. B.; Burdick, J. A.; Chen, C. S. Cell-mediated fibre recruitment drives extracellular matrix mechanosensing in engineered fibrillar microenvironments. *Nat. Mater.* **2015**, *14* (12), 1262−1268.

(33) Jain, P.; Nishiguchi, A.; Linz, G.; Wessling, M.; Ludwig, A.; Rossaint, R.; Möller, M.; Singh, S. Reconstruction of Ultra-thin Alveolar-capillary Basement Membrane Mimics. *Adv. Biol.* **2021**, *5* (8), 2000427.

(34) Slater, S. C.; Beachley, V.; Hayes, T.; Zhang, D.; Welsh, G. I.; Saleem, M. A.; Mathieson, P. W.; Wen, X.; Su, B.; Satchell, S. C. An in vitro model of the glomerular capillary wall using electrospun collagen nanofibres in a bioartificial composite basement membrane. *PLoS One* **2011**, *6* (6), e20802.

(35) Dorrello, N. V.; Vunjak-Novakovic, G. Bioengineering of pulmonary epithelium with preservation of the vascular niche. *Front. Bioeng. Biotechnol.* **2020**, *8*, 269.

(36) Doryab, A.; Taskin, M. B.; Stahlhut, P.; Schroppel, A.; Orak, S.; Voss, C.; Ahluwalia, A.; Rehberg, M.; Hilgendorff, A.; Stoger, T.; Groll, J.; Schmid, O. A bioinspired in vitro lung model to study particokinetics of nano-/microparticles under cyclic stretch and air-liquid interface conditions. *Front. Bioeng. Biotechnol.* **2021**, *9*, 616830.

(37) Fernández-Colino, A.; Iop, L.; Ferreira, M. S. V.; Mela, P. Fibrosis in tissue engineering and regenerative medicine: treat or trigger? *Adv. Drug Delivery Rev.* **2019**, *146*, 17−36.

(38) Huh, D.; Matthews, B. D.; Mammoto, A.; Montoya-Zavala, M.; Hsin, H. Y.; Ingber, D. E. Reconstituting organ-level lung functions on a chip. *Science* **2010**, *328* (5986), 1662−1668.

(39) Kim, I. L.; Mauck, R. L.; Burdick, J. A. Hydrogel design for cartilage tissue engineering: a case study with hyaluronic acid. *Biomaterials* **2011**, *32* (34), 8771−8782.

(40) Mollet, B. B.; Bogaerts, I. L.; van Almen, G. C.; Dankers, P. Y. A bioartificial environment for kidney epithelial cells based on a supramolecular polymer basement membrane mimic and an organo-typical culture system. *J. Tissue Eng. Regen. Med.* **2017**, *11* (6), 1820−1834.

(41) Nishiguchi, A.; Singh, S.; Wessling, M.; Kirkpatrick, C. J.; Möller, M. Basement membrane mimics of biofunctionalized nanofibers for a bipolar-cultured human primary alveolar-capillary barrier model. *Biomacromolecules* **2017**, *18* (3), 719−727.

(42) Nuttelman, C. R.; Tripodi, M. C.; Anseth, K. S. Synthetic hydrogel niches that promote hMSC viability. *Matrix Biol.* **2005**, *24* (3), 208−218.

(43) Sedláková, V.; Kloučková, M.; Garlíková, Z.; Vašíčková, K.; Jaroš, J.; Kandra, M.; Kotasová, H.; Hampl, A. Options for modeling the respiratory system: Inserts, scaffolds and microfluidic chips. *Drug Discovery Today* **2019**, *24* (4), 971−982.

(44) O'brien, F. J. Biomaterials & scaffolds for tissue engineering. *Mater. Today* **2011**, *14* (3), 88−95.

(45) Farquhar, M. G. The glomerular basement membrane. *Cell Biol. Extracell. Matrix* **1981**, *1981*, 335−378.

(46) Rhrissorrakrai, K.; Belcastro, V.; Bilal, E.; Norel, R.; Poussin, C.; Mathis, C.; Dulize, R. H.; Ivanov, N. V.; Alexopoulos, L.; Jeremy Rice, J.; et al. Understanding the limits of animal models as predictors of human biology: lessons learned from the sbv IMPROVER Species Translation Challenge. *Bioinformatics* **2015**, *31* (4), 471−483.

(47) Moran, C. J.; Ramesh, A.; Brama, P. A.; O'Byrne, J. M.; O'Brien, F. J.; Levingstone, T. J. The benefits and limitations of animal models for translational research in cartilage repair. *J. Exp. Orthop.* **2016**, *3*, 1.

(48) Brubaker, D. K.; Proctor, E. A.; Haigis, K. M.; Lauffenburger, D. A. Computational translation of genomic responses from experimental model systems to humans. *PLoS Comp. Biol.* **2019**, *15* (1), e1006286.

(49) Giovannetti, E.; Peters, G. Beyond animal models: implementing the 3Rs principles and improving pharmacological studies with new model systems. *Expert Opin. Drug Metab. Toxicol.* **2021**, *17* (8), 867−868.

(50) Porter, R.; Whelan, J. *Basement Membranes and Cell Movement*; Wiley: 2009.

(51) Leblond, C.; Inoue, S. Structure, composition, and assembly of basement membrane. *Dev. Dyn.* **1989**, *185* (4), 367−390.

(52) Rowe, R. G.; Weiss, S. J. Breaching the basement membrane: who, when and how? *Trends Cell Biol.* **2008**, *18* (11), 560−574.

(53) Merker, H. J. Morphology of the basement membrane. *Microsc. Res. Technol.* **1994**, *28* (2), 95−124.

(54) Sasaki, T.; Fässler, R.; Hohenester, E. Laminin: the crux of basement membrane assembly. *J. Cell Biol.* **2004**, *164* (7), 959−963.

(55) Kalluri, R. Basement membranes: structure, assembly and role in tumour angiogenesis. *Nat. Rev. Cancer* **2003**, *3* (6), 422−434.

(56) LeBleu, V. S.; MacDonald, B.; Kalluri, R. Structure and Function of Basement Membranes. *Experimental Biology and Medicine* **2007**, *232* (9), 1121−1129.

(57) Yurchenco, P. D. Basement membranes: cell scaffoldings and signaling platforms. *Cold Spring Harb. Perspect. Biol.* **2011**, *3* (2), a004911.

(58) Mao, M.; Alavi, M. V.; Labelle-Dumais, C.; Gould, D. B. Chapter Three-Type IV Collagens and Basement Membrane Diseases: Cell Biology and Pathogenic Mechanisms. *Curr. Top. Membr.* **2015**, *76*, 61−116.

(59) Timpl, R. Macromolecular organization of basement membranes. *Curr. Opin. Cell Biol.* **1996**, *8* (5), 618−624.

(60) Tunggal, P.; Smyth, N.; Paulsson, M.; Ott, M. C. Laminins: structure and genetic regulation. *Microsc. Res. Technol.* **2000**, *51* (3), 214−227.

(61) Paulsson, M. Basement membrane proteins: structure, assembly, and cellular interactions. *Crit. Rev. Biochem. Mol. Biol.* **1992**, *27* (1−2), 93−127.

(62) Kimura, N.; Toyoshima, T.; Kojima, T.; Shimane, M. Entactin-2: a new member of basement membrane protein with high homology to entactin/nidogen. *Exp. Cell Res.* **1998**, *241* (1), 36−45.

(63) AUMAILLEY, M.; WIEDEMANN, H.; MANN, K.; TIMPL, R. Binding of nidogen and the laminin-nidogen complex to basement membrane collagen type IV. *FEBS J.* **1989**, *184* (1), 241−248.

(64) French, M.; Smith, S.; Akanbi, K.; Sanford, T.; Hecht, J.; Farach-Carson, M.; Carson, D. Expression of the heparan sulfate proteoglycan, perlecan, during mouse embryogenesis and perlecan chondrogenic activity in vitro. *J. Cell Biol.* **1999**, *145* (5), 1103−1115.

(65) Reed, M. J.; Damodarasamy, M.; Banks, W. A. The extracellular matrix of the blood−brain barrier: structural and functional roles in health, aging, and Alzheimer's disease. *Tissue Barriers* **2019**, *7* (4), 1651157.

(66) Behrens, D. T.; Villone, D.; Koch, M.; Brunner, G.; Sorokin, L.; Robenek, H.; Bruckner-Tuderman, L.; Bruckner, P.; Hansen, U. The epidermal basement membrane is a composite of separate laminin-or collagen IV-containing networks connected by aggregated perlecan, but not by nidogens. *J. Biol. Chem.* **2012**, *287* (22), 18700−18709.

(67) Li, A.; Thompson, R. *Basement membrane components*. BMJ Publishing Group: 2003; Vol. *56*, pp 885−887.

(68) Pompili, S.; Latella, G.; Gaudio, E.; Sferra, R.; Vetuschi, A. The Charming World of the Extracellular Matrix: A Dynamic and Protective Network of the Intestinal Wall. *Front. Med.* **2021**, *8*, 477.

(69) Mutgan, A. C.; Jandl, K.; Kwapiszewska, G. Endothelial basement membrane components and their products, matrikines: active drivers of pulmonary hypertension? *Cells* **2020**, *9* (9), 2029.

(70) Matthes, S. A.; Hadley, R.; Roman, J.; White, E. S. Comparative biology of the normal lung extracellular matrix. In *Comparative biology of the normal lung*; Parent, R. A., Ed.; Elsevier: 2015; Vol. *2015*, pp 387−402.

(71) Miner, J. H. Glomerular basement membrane composition and the filtration barrier. *Pediatr. Nephrol.* **2011**, *26* (9), 1413−1417.

(72) Chen, C. H.; Hansma, H. G. Basement membrane macro-molecules: insights from atomic force microscopy. *J. Struct. Biol.* **2000**, *131* (1), 44−55.

(73) Farquhar, M. G. The glomerular basement membrane: not gone, just forgotten. *J. Clin. Invest.* **2006**, *116* (8), 2090−2093.

(74) Farquhar, M. G.; Wissig, S. L.; Palade, G. E. Glomerular permeability: I. Ferritin transfer across the normal glomerular capillary wall. *J. Exp. Med.* **1961**, *113* (1), 47−66.

(75) Iozzo, R. V. Basement membrane proteoglycans: from cellar to ceiling. *Nat. Rev. Mol. Cell Biol.* **2005**, *6* (8), 646−656.

(76) Whitelock, J. M.; Melrose, J.; Iozzo, R. V. Diverse cell signaling events modulated by perlecan. *Biochemistry* **2008**, *47* (43), 11174−11183.

(77) Bix, G.; Iozzo, R. V. Matrix revolutions:'tails' of basement-membrane components with angiostatic functions. *Trends Cell Biol.* **2005**, *15* (1), 52−60.

(78) Baird, A.; Ling, N. Fibroblast growth factors are present in the extracellular matrix produced by endothelial cells invitro: Implications for a role of heparinase-like enzymes in the neovascular response. *Biochem. Biophys. Res. Commun.* **1987**, *142* (2), 428−435.

(79) Bashkin, P.; Doctrow, S.; Klagsbrun, M.; Svahn, C. M.; Folkman, J.; Vlodavsky, I. Basic fibroblast growth factor binds to subendothelial extracellular matrix and is released by heparitinase and heparin-like molecules. *Biochemistry* **1989**, *28* (4), 1737−1743.

(80) Folkman, J.; Klagsbrun, M.; Sasse, J.; Wadzinski, M.; Ingber, D.; Vlodavsky, I. A heparin-binding angiogenic protein–basic fibroblast growth factor–is stored within basement membrane. *Am. J. Pathol.* **1988**, *130* (2), 393.

(81) Saksela, O.; Moscatelli, D.; Sommer, A.; Rifkin, D. B. Endothelial cell-derived heparan sulfate binds basic fibroblast growth factor and protects it from proteolytic degradation. *J. Cell Biol.* **1988**, *107* (2), 743−751.

(82) Vlodavsky, I.; Folkman, J.; Sullivan, R.; Fridman, R.; Ishai-Michaeli, R.; Sasse, J.; Klagsbrun, M. Endothelial cell-derived basic fibroblast growth factor: synthesis and deposition into subendothelial extracellular matrix. *Proc. Natl. Acad. Sci. U. S. A.* **1987**, *84* (8), 2292−2296.

(83) Vukicevic, S.; Kleinman, H. K.; Luyten, F. P.; Roberts, A. B.; Roche, N. S.; Reddi, A. H. Identification of multiple active growth factors in basement membrane Matrigel suggests caution in interpretation of cellular activity related to extracellular matrix components. *Exp. Cell Res.* **1992**, *202* (1), 1−8.

(84) Li, J.; Zhang, Y. P.; Kirsner, R. S. Angiogenesis in wound repair: angiogenic growth factors and the extracellular matrix. *Microsc. Res. Technol.* **2003**, *60* (1), 107−114.

(85) Sund, M.; Xie, L.; Kalluri, R. The contribution of vascular basement membranes and extracellular matrix to the mechanics of tumor angiogenesis. *APMIS* **2004**, *112* (7−8), 450−462.

(86) Iozzo, R. V.; San Antonio, J. D. Heparan sulfate proteoglycans: heavy hitters in the angiogenesis arena. *J. Clin. Invest.* **2001**, *108* (3), 349−355.

(87) Ortega, N.; Werb, Z. New functional roles for non-collagenous domains of basement membrane collagens. *J. Cell Sci.* **2002**, *115* (22), 4201−4214.

(88) Oguro, K.; Kazama, T.; Isemura, M.; Nakamura, T.; Akai, S.; Sato, Y. Immunohistochemical alterations in basement membrane components of squamous cell carcinoma. *J. Invest. Dermatol.* **1991**, *96* (2), 250−254.

(89) Brody, S.; Anilkumar, T.; Liliensiek, S.; Last, J. A.; Murphy, C. J.; Pandit, A. Characterizing nanoscale topography of the aortic heart valve basement membrane for tissue engineering heart valve scaffold design. *Tissue Eng.* **2006**, *12* (2), 413−421.

(90) Janson, I. A.; Putnam, A. J. Extracellular matrix elasticity and topography: Material-based cues that affect cell function via conserved mechanisms. *J. Biomed. Mater. Res., Part A* **2015**, *103* (3), 1246−1258.

(91) Liliensiek, S. J.; Nealey, P.; Murphy, C. J. Characterization of endothelial basement membrane nanotopography in rhesus macaque as a guide for vessel tissue engineering. *Tissue Eng., Part A* **2009**, *15* (9), 2643−2651.

(92) Kulangara, K.; Leong, K. W. Substrate topography shapes cell function. *Soft Matter* **2009**, *5* (21), 4072−4076.

(93) Bettinger, C. J.; Langer, R.; Borenstein, J. T. Engineering substrate topography at the micro-and nanoscale to control cell function. *Angew. Chem., Int. Ed.* **2009**, *48* (30), 5406−5415.

(94) Davis, K. A.; Burke, K. A.; Mather, P. T.; Henderson, J. H. Dynamic cell behavior on shape memory polymer substrates. *Biomaterials* **2011**, *32* (9), 2285−2293.

(95) Ross, A. M.; Jiang, Z.; Bastmeyer, M.; Lahann, J. Physical aspects of cell culture substrates: topography, roughness, and elasticity. *Small* **2012**, *8* (3), 336−355.

(96) Mascharak, S.; Benitez, P. L.; Proctor, A. C.; Madl, C. M.; Hu, K. H.; Dewi, R. E.; Butte, M. J.; Heilshorn, S. C. YAP-dependent mechanotransduction is required for proliferation and migration on native-like substrate topography. *Biomaterials* **2017**, *115*, 155−166.

(97) Yang, M. T.; Fu, J.; Wang, Y.-K.; Desai, R. A.; Chen, C. S. Assaying stem cell mechanobiology on microfabricated elastomeric substrates with geometrically modulated rigidity. *Nat. Protoc.* **2011**, *6* (2), 187.

(98) Last, J. A.; Liliensiek, S. J.; Nealey, P. F.; Murphy, C. J. Determining the mechanical properties of human corneal basement membranes with atomic force microscopy. *J. Struct. Biol.* **2009**, *167* (1), 19−24.

(99) Welling, L. W.; Grantham, J. J. Physical properties of isolated perfused renal tubules and tubular basement membranes. *J. Clin. Invest.* **1972**, *51* (5), 1063−1075.

(100) Soofi, S. S.; Last, J. A.; Liliensiek, S. J.; Nealey, P. F.; Murphy, C. J. The elastic modulus of Matrigel as determined by atomic force microscopy. *J. Struct. Biol.* **2009**, *167* (3), 216−219.

(101) Danielsen, C. C. Tensile mechanical and creep properties of Descemet's membrane and lens capsule. *Exp. Eye Res.* **2004**, *79* (3), 343−350.

(102) Biela, S. A.; Su, Y.; Spatz, J. P.; Kemkemer, R. Different sensitivity of human endothelial cells, smooth muscle cells and fibroblasts to topography in the nano−micro range. *Acta Biomater.* **2009**, *5* (7), 2460−2466.

(103) Dreier, B.; Gasiorowski, J. Z.; Morgan, J. T.; Nealey, P. F.; Russell, P.; Murphy, C. J. Early responses of vascular endothelial cells to topographic cues. *Am. J. Physiol.: Cell Physiol.* **2013**, *305* (3), C290−C298.

(104) Liliensiek, S. J.; Campbell, S.; Nealey, P. F.; Murphy, C. J. The scale of substratum topographic features modulates proliferation of corneal epithelial cells and corneal fibroblasts. *J. Biomed. Mater. Res., Part A* **2006**, *79A* (1), 185−192.

(105) Liliensiek, S. J.; Wood, J. A.; Yong, J.; Auerbach, R.; Nealey, P. F.; Murphy, C. J. Modulation of human vascular endothelial cell behaviors by nanotopographic cues. *Biomaterials* **2010**, *31* (20), 5418−5426.

(106) Abrams, G.; Goodman, S.; Nealey, P.; Franco, M.; Murphy, C. J. Nanoscale topography of the basement membrane underlying the corneal epithelium of the rhesus macaque. *Cell Tissue Res.* **2000**, *299* (1), 39−46.

(107) Abrams, G. A.; Murphy, C. J.; Wang, Z.-Y.; Nealey, P. F.; Bjorling, D. E. Ultrastructural basement membrane topography of the bladder epithelium. *Urol. Res.* **2003**, *31* (5), 341−346.

(108) Fabris, G.; Lucantonio, A.; Hampe, N.; Noetzel, E.; Hoffmann, B.; DeSimone, A.; Merkel, R. Nanoscale Topography and Poroelastic Properties of Model Tissue Breast Gland Basement Membranes. *Biophys. J.* **2018**, *115* (9), 1770−1782.

(109) Morrissey, M. A.; Sherwood, D. R. An active role for basement membrane assembly and modification in tissue sculpting. *J. Cell Sci.* **2015**, *128* (9), 1661−1668.

(110) Li, Y.; Zhu, Y.; Yu, H.; Chen, L.; Liu, Y. Topographic characterization and protein quantification of esophageal basement membrane for scaffold design reference in tissue engineering. *J. Biomed. Mater. Res. B Appl. Biomater.* **2012**, *100B* (1), 265−273.

(111) Sherwood, D. R. Cell invasion through basement membranes: an anchor of understanding. *Trends Cell Biol.* **2006**, *16* (5), 250−256.

(112) Huber, A. R.; Weiss, S. J. Disruption of the subendothelial basement membrane during neutrophil diapedesis in an in vitro construct of a blood vessel wall. *J. Clin. Invest.* **1989**, *83* (4), 1122.

(113) Ley, K.; Laudanna, C.; Cybulsky, M. I.; Nourshargh, S. Getting to the site of inflammation: the leukocyte adhesion cascade updated. *Nat. Rev. Immunol.* **2007**, *7* (9), 678−689.

(114) Srivastava, A.; Pastor-Pareja, J. C.; Igaki, T.; Pagliarini, R.; Xu, T. Basement membrane remodeling is essential for Drosophila disc eversion and tumor invasion. *Proc. Natl. Acad. Sci. U. S. A.* **2007**, *104* (8), 2721−2726.

(115) Hotary, K.; Li, X.-Y.; Allen, E.; Stevens, S. L.; Weiss, S. J. A cancer cell metalloprotease triad regulates the basement membrane transmigration program. *Genes Dev.* **2006**, *20* (19), 2673−2686.

(116) Howat, W. J.; Holmes, J. A.; Holgate, S. T.; Lackie, P. M. Basement membrane pores in human bronchial epithelium: a conduit for infiltrating cells? *Am. J. Pathol.* **2001**, *158* (2), 673−680.

(117) Gautam, M.; Noakes, P. G.; Moscoso, L.; Rupp, F.; Scheller, R. H.; Merlie, J. P.; Sanes, J. R. Defective neuromuscular synaptogenesis in agrin-deficient mutant mice. *Cell* **1996**, *85* (4), 525−535.

(118) Fukai, N.; Eklund, L.; Marneros, A. G.; Oh, S. P.; Keene, D. R.; Tamarkin, L.; Niemelä, M.; Ilves, M.; Li, E.; Pihlajaniemi, T. Lack of collagen XVIII/endostatin results in eye abnormalities. *EMBO J.* **2002**, *21* (7), 1535−1544.

(119) Wyss, H. M.; Henderson, J. M.; Byfield, F. J.; Bruggeman, L. A.; Ding, Y.; Huang, C.; Suh, J. H.; Franke, T.; Mele, E.; Pollak, M. R.; et al. Biophysical properties of normal and diseased renal glomeruli. *Am. J. Physiol.: Cell Physiol.* **2011**, *300* (3), C397−C405.

(120) Thomsen, M. S.; Routhe, L. J.; Moos, T. The vascular basement membrane in the healthy and pathological brain. *J. Cereb. Blood Flow Metab.* **2017**, *37* (10), 3300−3317.

(121) Halfter, W.; Moes, S.; Asgeirsson, D. O.; Halfter, K.; Oertle, P.; Melo Herraiz, E.; Plodinec, M.; Jenoe, P.; Henrich, P. B. Diabetes-related changes in the protein composition and the biomechanical properties of human retinal vascular basement membranes. *PLoS One* **2017**, *12* (12), e0189857.

(122) Candiello, J.; Cole, G. J.; Halfter, W. Age-dependent changes in the structure, composition and biophysical properties of a human basement membrane. *Matrix Biol.* **2010**, *29* (5), 402−410.

(123) Han, F.; Wang, J.; Ding, L.; Hu, Y.; Li, W.; Yuan, Z.; Guo, Q.; Zhu, C.; Yu, L.; Wang, H.; et al. Tissue Engineering and Regenerative Medicine: Achievements, Future, and Sustainability in Asia. *Front. Bioeng. Biotechnol.* **2020**, *8*, 83.

(124) Zeng, Y.; Yang, J.; Huang, K.; Lee, Z.; Lee, X. A comparison of biomechanical properties between human and porcine cornea. *J. Biomech.* **2001**, *34* (4), 533−537.

(125) Fisher, R.; Wakely, J. The elastic constants and ultrastructural organization of a basement membrane (lens capsule). *Proc. R. Soc. London B. Biol. Sci.* **1976**, *193* (1113), 335−358.

(126) Thomasy, S. M.; Raghunathan, V. K.; Winkler, M.; Reilly, C. M.; Sadeli, A. R.; Russell, P.; Jester, J. V.; Murphy, C. J. Elastic modulus and collagen organization of the rabbit cornea: epithelium to endothelium. *Acta Biomater.* **2014**, *10* (2), 785−791.

(127) Liu, Z.; Ji, J.; Zhang, J.; Huang, C.; Meng, Z.; Qiu, W.; Li, X.; Wang, W. Corneal reinforcement using an acellular dermal matrix for an analysis of biocompatibility, mechanical properties, and transparency. *Acta Biomater.* **2012**, *8* (9), 3326−3332.

(128) Maina, J. N. Morphological and morphometric properties of the blood-gas barrier: comparative perspectives. In *The Vertebrate Blood-Gas Barrier in Health and Disease*; Makanya, A. N., Ed.; Springer: 2015; Vol. *2015*, pp 15−38.

(129) Hinderer, S.; Layland, S. L.; Schenke-Layland, K. ECM and ECM-like materials—Biomaterials for applications in regenerative medicine and cancer therapy. *Adv. Drug Delivery Rev.* **2016**, *97*, 260−269.

(130) Richbourg, N. R.; Peppas, N. A.; Sikavitsas, V. I. Tuning the biomimetic behavior of scaffolds for regenerative medicine through surface modifications. *J. Tissue Eng. Regen. Med.* **2019**, *13* (8), 1275−1293.

(131) Stratton, S.; Shelke, N. B.; Hoshino, K.; Rudraiah, S.; Kumbar, S. G. Bioactive polymeric scaffolds for tissue engineering. *Bioact. Mater.* **2016**, *1* (2), 93−108.

(132) Beningo, K. A.; Wang, Y.-L. Flexible substrata for the detection of cellular traction forces. *Trends Cell Biol.* **2002**, *12* (2), 79−84.

(133) Cao, L.; Mooney, D. J. Spatiotemporal control over growth factor signaling for therapeutic neovascularization. *Adv. Drug Delivery Rev.* **2007**, *59* (13), 1340−1350.

(134) Ingber, D. E.; Whitesides, G. M. Patterning proteins and cells using soft lithography. *Biomaterials* **2011**, *20*, 2363.

(135) Lee, C. H.; Shin, H. J.; Cho, I. H.; Kang, Y.-M.; Kim, I. A.; Park, K.-D.; Shin, J.-W. Nanofiber alignment and direction of mechanical strain affect the ECM production of human ACL fibroblast. *Biomaterials* **2005**, *26* (11), 1261−1270.

(136) Lehnert, D.; Wehrle-Haller, B.; David, C.; Weiland, U.; Ballestrem, C.; Imhof, B. A.; Bastmeyer, M. Cell behaviour on micropatterned substrata: limits of extracellular matrix geometry for spreading and adhesion. *J. Cell Sci.* **2004**, *117* (1), 41−52.

(137) Xia, Y.; Whitesides, G. M. Soft lithography. *Annu. Rev. Mater. Sci.* **1998**, *28* (1), 153−184.

(138) Gelain, F.; Bottai, D.; Vescovi, A.; Zhang, S. Designer self-assembling peptide nanofiber scaffolds for adult mouse neural stem cell 3-dimensional cultures. *PLoS One* **2006**, *1* (1), e119.

(139) Ura, D. P.; Karbowniczek, J. E.; Szewczyk, P. K.; Metwally, S.; Kopyściański, M.; Stachewicz, U. Cell integration with electrospun PMMA nanofibers, microfibers, ribbons, and films: a microscopy study. *Bioengineering* **2019**, *6* (2), 41.

(140) Wahl, E. A.; Fierro, F. A.; Peavy, T. R.; Hopfner, U.; Dye, J. F.; Machens, H.-G.; Egaña, J. T.; Schenck, T. L. In Vitro Evaluation of Scaffolds for the Delivery of Mesenchymal Stem Cells to Wounds. *BioMed. Res. Int.* **2015**, *2015*, 108571.

(141) George, J. H.; Nagel, D.; Waller, S.; Hill, E.; Parri, H. R.; Coleman, M. D.; Cui, Z.; Ye, H. A closer look at neuron interaction with track-etched microporous membranes. *Sci. Rep.* **2018**, *8*, 15552.

(142) Kim, M. Y.; Li, D. J.; Pham, L. K.; Wong, B. G.; Hui, E. E. Microfabrication of high-resolution porous membranes for cell culture. *J. Membr. Sci.* **2014**, *452*, 460−469.

(143) Zheng, F.; Li, Q.; Yang, P.; Qiu, S.; Mao, H.; Zhao, J. *Fabrication of Ultra-Thin Micro-Porous PDMS Membrane for Cell Co-Culture in Blood Brain Barrier Model on Chip*, 2021 21st International Conference on Solid-State Sensors, Actuators and Microsystems (Transducers), IEEE: 2021; pp 279−282.

(144) Zakharova, M.; Palma do Carmo, M. A.; van der Helm, M. W.; Le-The, H.; de Graaf, M. N. S.; Orlova, V.; van den Berg, A.; van der Meer, A. D.; Broersen, K.; Segerink, L. I. Multiplexed blood−brain barrier organ-on-chip. *Lab Chip* **2020**, *20* (17), 3132−3143.

(145) Douville, N. J.; Tung, Y.-C.; Li, R.; Wang, J. D.; El-Sayed, M. E.; Takayama, S. Fabrication of two-layered channel system with embedded electrodes to measure resistance across epithelial and endothelial barriers. *Anal. Chem.* **2010**, *82* (6), 2505−2511.

(146) Shrestha, J.; Razavi Bazaz, S.; Aboulkheyr Es, H.; Yaghobian Azari, D.; Thierry, B.; Ebrahimi Warkiani, M.; Ghadiri, M. Lung-on-a-chip: the future of respiratory disease models and pharmacological studies. *Crit. Rev. Biotechnol.* **2020**, *40* (2), 213−230.

(147) Huh, D.; Leslie, D. C.; Matthews, B. D.; Fraser, J. P.; Jurek, S.; Hamilton, G. A.; Thorneloe, K. S.; McAlexander, M. A.; Ingber, D. E. A human disease model of drug toxicity−induced pulmonary edema in a lung-on-a-chip microdevice. *Sci. Transl. Med.* **2012**, *4* (159), 159ra147−159ra147.

(148) Quirós-Solano, W.; Gaio, N.; Stassen, O.; Arik, Y.; Silvestri, C.; Van Engeland, N.; Van der Meer, A.; Passier, R.; Sahlgren, C.; Bouten, C.; et al. Microfabricated tuneable and transferable porous PDMS membranes for Organs-on-Chips. *Sci. Rep.* **2018**, *8*, 13524.

(149) Stucki, J. D.; Hobi, N.; Galimov, A.; Stucki, A. O.; Schneider-Daum, N.; Lehr, C.-M.; Huwer, H.; Frick, M.; Funke-Chambour, M.; Geiser, T.; Guenat, O. T. Medium throughput breathing human primary cell alveolus-on-chip model. *Sci. Rep.* **2018**, *8*, 14359.

(150) Zakharova, M.; Tibbe, M. P.; Koch, L. S.; Le-The, H.; Leferink, A. M.; den Berg, A.; Meer, A. D.; Broersen, K.; Segerink, L. I. Transwell-Integrated 2 μm Thick Transparent Polydimethylsiloxane Membranes with Controlled Pore Sizes and Distribution to Model the Blood-Brain Barrier. *Adv. Mater. Technol.* **2021**, *6* (12), 2100138.

(151) Chuah, Y. J.; Kuddannaya, S.; Lee, M. H. A.; Zhang, Y.; Kang, Y. The effects of poly (dimethylsiloxane) surface silanization on the mesenchymal stem cell fate. *Biomater. Sci.* **2015**, *3* (2), 383−390.

(152) Wang, J. D.; Douville, N. J.; Takayama, S.; ElSayed, M. Quantitative analysis of molecular absorption into PDMS microfluidic channels. *Ann. Biomed. Eng.* **2012**, *40* (9), 1862−1873.

(153) Yonker, L. M.; Mou, H.; Chu, K. K.; Pazos, M. A.; Leung, H.; Cui, D.; Ryu, J.; Hibbler, R. M.; Eaton, A. D.; Ford, T. N.; et al. Development of a primary human co-culture model of inflamed airway mucosa. *Sci. Rep.* **2017**, *7*, 8182.

(154) Levardon, H.; Yonker, L. M.; Hurley, B. P.; Mou, H. Expansion of airway basal cells and generation of polarized epithelium. *Bio-protocol* **2018**, *8* (11), e2877.

(155) Kang, Y. B. A.; Rawat, S.; Cirillo, J.; Bouchard, M.; Noh, H. M. Layered long-term co-culture of hepatocytes and endothelial cells on a transwell membrane: toward engineering the liver sinusoid. *Biofabrication* **2013**, *5* (4), 045008.

(156) Hatherell, K.; Couraud, P.-O.; Romero, I. A.; Weksler, B.; Pilkington, G. J. Development of a three-dimensional, all-human in vitro model of the blood−brain barrier using mono-, co-, and tri-cultivation Transwell models. *J. Neurosci. Methods* **2011**, *199* (2), 223−229.

(157) Antunes, F.; Andrade, F.; Araújo, F.; Ferreira, D.; Sarmento, B. Establishment of a triple co-culture in vitro cell models to study intestinal absorption of peptide drugs. *Eur. J. Pharm. Biopharm.* **2013**, *83* (3), 427−435.

(158) Kasper, J.; Hermanns, M. I.; Bantz, C.; Maskos, M.; Stauber, R.; Pohl, C.; Unger, R. E.; Kirkpatrick, J. C. Inflammatory and cytotoxic responses of an alveolar-capillary coculture model to silica nanoparticles: comparison with conventional monocultures. *Part. Fibre Toxicol.* **2011**, *8* (1), 6.

(159) Hermanns, M. I.; Unger, R. E.; Kehe, K.; Peters, K.; Kirkpatrick, C. J. Lung epithelial cell lines in coculture with human pulmonary microvascular endothelial cells: development of an alveolo-capillary barrier in vitro. *Lab. Invest.* **2004**, *84* (6), 736−752.

(160) Kim, Y.; Park, N.; Rim, Y. A.; Nam, Y.; Jung, H.; Lee, K.; Ju, J. H. Establishment of a complex skin structure via layered co-culture of keratinocytes and fibroblasts derived from induced pluripotent stem cells. *Stem Cell. Res. Ther.* **2018**, *9*, 217.

(161) Pasman, T.; Grijpma, D.; Stamatialis, D.; Poot, A. Flat and microstructured polymeric membranes in organs-on-chips. *J. R Soc. Interface* 2018, 15 (144), 20180351.

(162) Kasper, J.; Hermanns, M. I.; Bantz, C.; Maskos, M.; Stauber, R.; Pohl, C.; Unger, R. E.; Kirkpatrick, J. C. Inflammatory and cytotoxic responses of an alveolar-capillary coculture model to silica nanoparticles: comparison with conventional monocultures. *Part. Fibre Toxicol.* 2011, 8, 6.

(163) Di Cio, S.; Gautrot, J. E. Cell sensing of physical properties at the nanoscale: Mechanisms and control of cell adhesion and phenotype. *Acta Biomater.* 2016, 30, 26–48.

(164) Lu, Q.; Yin, H.; Grant, M. P.; Elisseeff, J. H. An in vitro model for the ocular surface and tear film system. *Sci. Rep.* 2017, 7 (1), 6163.

(165) Chakraborty, S.; Winkelmann, V. E.; Braumuller, S.; Palmer, A.; Schultze, A.; Klohs, B.; Ignatius, A.; Vater, A.; Fauler, M.; Frick, M.; Huber-Lang, M. Role of the C5a-C5a receptor axis in the inflammatory responses of the lungs after experimental polytrauma and hemorrhagic shock. *Sci. Rep.* 2021, 11 (1), 2158.

(166) Cruz-Acuña, R.; García, A. J. Synthetic hydrogels mimicking basement membrane matrices to promote cell-matrix interactions. *Matrix Biol.* 2017, 57, 324–333.

(167) Janmey, P. A.; Winer, J. P.; Weisel, J. W. Fibrin gels and their clinical and bioengineering applications. *J. R. Soc., Interface* 2009, 6 (30), 1–10.

(168) Lee, K. Y.; Mooney, D. J. Alginate: properties and biomedical applications. *Prog. Polym. Sci.* 2012, 37 (1), 106–126.

(169) Matricardi, P.; Di Meo, C.; Coviello, T.; Hennink, W. E.; Alhaique, F. Interpenetrating polymer networks polysaccharide hydrogels for drug delivery and tissue engineering. *Adv. Drug Delivery Rev.* 2013, 65 (9), 1172–1187.

(170) Aamodt, J. M.; Grainger, D. W. Extracellular matrix-based biomaterial scaffolds and the host response. *Biomaterials* 2016, 86, 68–82.

(171) Rijal, G. The decellularized extracellular matrix in regenerative medicine. *Regenerative Medicine* 2017, 12 (5), 475–477.

(172) Benton, G.; Arnaoutova, I.; George, J.; Kleinman, H. K.; Koblinski, J. Matrigel: from discovery and ECM mimicry to assays and models for cancer research. *Adv. Drug Delivery Rev.* 2014, 79, 3–18.

(173) Johnson, D. L.; Scott, R.; Newman, R. Pluripotent stem cell culture scale-out. *Assay Guidance Manual [Internet]* 2021. See the following: https://www.ncbi.nlm.nih.gov/books/NBK571710/.

(174) Sato, T.; Vries, R. G.; Snippert, H. J.; van de Wetering, M.; Barker, N.; Stange, D. E.; van Es, J. H.; Abo, A.; Kujala, P.; Peters, P. J.; Clevers, H. Single Lgr5 stem cells build crypt-villus structures in vitro without a mesenchymal niche. *Nature* 2009, 459 (7244), 262–265.

(175) Pham, M. T.; Pollock, K. M.; Rose, M. D.; Cary, W. A.; Stewart, H. R.; Zhou, P.; Nolta, J. A.; Waldau, B. Generation of human vascularized brain organoids. *Neuroreport* 2018, 29 (7), 588.

(176) Hocevar, S. E.; Liu, L.; Duncan, R. K. Matrigel is required for efficient differentiation of isolated, stem cell-derived otic vesicles into inner ear organoids. *Stem Cell Res.* 2021, 53, 102295.

(177) Choo, N.; Ramm, S.; Luu, J.; Winter, J. M.; Selth, L. A.; Dwyer, A. R.; Frydenberg, M.; Grummet, J.; Sandhu, S.; Hickey, T. E.; et al. High-throughput imaging assay for drug screening of 3D prostate cancer organoids. *SLAS Discovery* 2021, 26 (9), 1107–1124.

(178) Tas, S.; Bölükbas, D. A.; Alsafadi, H. N.; Da Silva, I. A.; De Santis, M. M.; Rehnberg, E.; Tamargo, I.; Mohlin, S.; Lindstedt, S.; Wagner, D. E. Decellularized extracellular matrix hydrogels for human airway organoid culture. *ERJ. Open Res.* 2021, 7 (suppl 6), 101.

(179) Hughes, C. S.; Postovit, L. M.; Lajoie, G. A. Matrigel: a complex protein mixture required for optimal growth of cell culture. *Proteomics* 2010, 10 (9), 1886–1890.

(180) Aisenbrey, E. A.; Murphy, W. L. Synthetic alternatives to Matrigel. *Nat. Rev. Mater.* 2020, 5 (7), 539–551.

(181) Van Hemelryk, A.; Mout, L.; Erkens-Schulze, S.; French, P. J.; van Weerden, W. M.; van Royen, M. E. Modeling Prostate Cancer Treatment Responses in the Organoid Era: 3D Environment Impacts Drug Testing. *Biomolecules* 2021, 11 (11), 1572.

(182) Nikolaev, M.; Mitrofanova, O.; Broguiere, N.; Geraldo, S.; Dutta, D.; Tabata, Y.; Elci, B.; Brandenberg, N.; Kolotuev, I.; Gjorevski, N.; et al. Homeostatic mini-intestines through scaffold-guided organoid morphogenesis. *Nature* 2020, 585 (7826), 574–578.

(183) Patel, B.; Wonski, B. T.; Saliganan, D. M.; Rteil, A.; Kabbani, L. S.; Lam, M. T. Decellularized dermis extracellular matrix alloderm mechanically strengthens biological engineered tunica adventitia-based blood vessels. *Sci. Rep.* 2021, 11, 11384.

(184) Young, B. M.; Antczak, L.-A. M.; Shankar, K.; Heise, R. L. A Two-Step Bioreactor for Decellularized Lung Epithelialization. *Cells Tissues Organs* 2021, 210 (4), 301–310.

(185) da Mata Martins, T. M.; da Silva Cunha, P.; Rodrigues, M. A.; de Carvalho, J. L.; de Souza, J. E.; de Carvalho Oliveira, J. A.; Gomes, D. A.; de Goes, A. M. Epithelial basement membrane of human decellularized cornea as a suitable substrate for differentiation of embryonic stem cells into corneal epithelial-like cells. *Mater. Sci. Eng., C* 2020, 116, 111215.

(186) Moreno-Manzano, V.; Zaytseva-Zotova, D.; López-Mocholí, E.; Briz-Redón, Á.; Løkensgard Strand, B.; Serrano-Aroca, Á. Injectable gel form of a decellularized bladder induces adipose-derived stem cell differentiation into smooth muscle cells in vitro. *Int. J. Mol. Sci.* 2020, 21 (22), 8608.

(187) Sobreiro-Almeida, R.; Gómez-Florit, M.; Quinteira, R.; Reis, R. L.; Gomes, M. E.; Neves, N. M. Decellularized kidney extracellular matrix bioinks recapitulate renal 3D microenvironment in vitro. *Biofabrication* 2021, 13 (4), 045006.

(188) Kakabadze, Z.; Kakabadze, A.; Chakhunashvili, D.; Karalashvili, L.; Berishvili, E.; Sharma, Y.; Gupta, S. Decellularized human placenta supports hepatic tissue and allows rescue in acute liver failure. *Hepatology* 2018, 67 (5), 1956–1969.

(189) Wang, C.; Li, G.; Cui, K.; Chai, Z.; Huang, Z.; Liu, Y.; Chen, S.; Huang, H.; Zhang, K.; Han, Z.; et al. Sulfated glycosaminoglycans in decellularized placenta matrix as critical regulators for cutaneous wound healing. *Acta Biomater.* 2021, 122, 199–210.

(190) Salah, R. A.; Mohamed, I. K.; El-Badri, N. Development of decellularized amniotic membrane as a bioscaffold for bone marrow-derived mesenchymal stem cells: ultrastructural study. *J. Mol. Histol.* 2018, 49 (3), 289–301.

(191) Villamil Ballesteros, A. C.; Segura Puello, H. R.; Lopez-Garcia, J. A.; Bernal-Ballen, A.; Nieto Mosquera, D. L.; Munoz Forero, D. M.; Segura Charry, J. S.; Neira Bejarano, Y. A. Bovine decellularized amniotic membrane: Extracellular matrix as scaffold for mammalian skin. *Polymers* 2020, 12 (3), 590.

(192) Yang, Y.; Zhang, Y.; Yan, Y.; Ji, Q.; Dai, Y.; Jin, S.; Liu, Y.; Chen, J.; Teng, L. A sponge-like double-layer wound dressing with chitosan and decellularized bovine amniotic membrane for promoting diabetic wound healing. *Polymers* 2020, 12 (3), 535.

(193) Xia, C.; Mei, S.; Gu, C.; Zheng, L.; Fang, C.; Shi, Y.; Wu, K.; Lu, T.; Jin, Y.; Lin, X.; Chen, P. Decellularized cartilage as a prospective scaffold for cartilage repair. *Mater. Sci. Eng., C* 2019, 101, 588–595.

(194) Mohiuddin, O. A.; Campbell, B.; Poche, J. N.; Thomas-Porch, C.; Hayes, D. A.; Bunnell, B. A.; Gimble, J. M. Decellularized adipose tissue: biochemical composition, in vivo analysis and potential clinical applications. *Cell Biology and Translational Medicine* 2019, 1212, 57–70.

(195) Wang, F.; Maeda, Y.; Zachar, V.; Ansari, T.; Emmersen, J. Regeneration of the oesophageal muscle layer from oesophagus acellular matrix scaffold using adipose-derived stem cells. *Biochem. Biophys. Res. Commun.* 2018, 503 (1), 271–277.

(196) Lu, S.; Cuzzucoli, F.; Jiang, J.; Liang, L.-G.; Wang, Y.; Kong, M.; Zhao, X.; Cui, W.; Li, J.; Wang, S. Development of a biomimetic liver tumor-on-a-chip model based on decellularized liver matrix for toxicity testing. *Lab Chip* 2018, 18 (22), 3379–3392.

(197) Doornaert, M.; Depypere, B.; Creytens, D.; Declercq, H.; Taminau, J.; Lemeire, K.; Monstrey, S.; Berx, G.; Blondeel, P. Human decellularized dermal matrix seeded with adipose-derived stem cells enhances wound healing in a murine model: Experimental study. *Ann. Med. Surg.* 2019, 46, 4–11.

(198) Wildman, D. E. Toward an integrated evolutionary understanding of the mammalian placenta. *Placenta* **2011**, *32*, S142–S145.

(199) Lobo, S. E.; Leonel, L. C. P.; Miranda, C. M.; Coelho, T. M.; Ferreira, G. A.; Mess, A.; Abrão, M. S.; Miglino, M. A. The placenta as an organ and a source of stem cells and extracellular matrix: a review. *Cells Tissues Organs* **2016**, *201* (4), 239–252.

(200) Amenta, P. S.; Gay, S.; Vaheri, A.; Martinez-Hernandez, A. The extracellular matrix is an integrated unit: ultrastructural localization of collagen types I, III, IV, V, VI, fibronectin, and laminin in human term placenta. *Coll. Relat. Res.* **1986**, *6* (2), 125–152.

(201) Zhang, X.; Xiao, S.; Liu, B.; Miao, Y.; Hu, Z. Use of extracellular matrix hydrogel from human placenta to restore hair-inductive potential of dermal papilla cells. *Regen. Med.* **2019**, *14* (8), 741–751.

(202) Rameshbabu, A. P.; Bankoti, K.; Datta, S.; Subramani, E.; Apoorva, A.; Ghosh, P.; Jana, S.; Manchikanti, P.; Roy, S.; Chaudhury, K.; Dhara, S. Bioinspired 3D porous human placental derived extracellular matrix/silk fibroin sponges for accelerated bone regeneration. *Mater. Sci. Eng., C* **2020**, *113*, 110990.

(203) Elkhenany, H.; El-Derby, A.; Abd Elkodous, M.; Salah, R. A.; Lotfy, A.; El-Badri, N. Applications of the amniotic membrane in tissue engineering and regeneration: the hundred-year challenge. *Stem Cell. Res. Ther.* **2022**, *13*, 8.

(204) Nasiry, D.; Khalatbary, A. R.; Abdollahifar, M.-A.; Amini, A.; Bayat, M.; Noori, A.; Piryaei, A. Engraftment of bioengineered three-dimensional scaffold from human amniotic membrane-derived extracellular matrix accelerates ischemic diabetic wound healing. *Arch. Dermatol. Res.* **2021**, *313* (7), 567–582.

(205) Jerman, U. D.; Veranič, P.; Kreft, M. E. Amniotic membrane scaffolds enable the development of tissue-engineered urothelium with molecular and ultrastructural properties comparable to that of native urothelium. *Tissue Eng., Part C* **2014**, *20* (4), 317–327.

(206) Ghorbani, F.; Abdihaji, M.; Roudkenar, M. H.; Ebrahimi, A. Development of a Cell-Based Biosensor for Residual Detergent Detection in Decellularized Scaffolds. *ACS Synth. Biol.* **2021**, *10* (10), 2715–2724.

(207) Yang, D.; Xiao, J.; Wang, B.; Li, L.; Kong, X.; Liao, J. The immune reaction and degradation fate of scaffold in cartilage/bone tissue engineering. *Mater. Sci. Eng., C* **2019**, *104*, 109927.

(208) Johnson, T. D.; Hill, R. C.; Dzieciatkowska, M.; Nigam, V.; Behfar, A.; Christman, K. L.; Hansen, K. C. Quantification of decellularized human myocardial matrix: a comparison of six patients. *Prot. Clin. Appl.* **2016**, *10* (1), 75–83.

(209) Bruyneel, A. A.; Carr, C. A. Ambiguity in the presentation of decellularized tissue composition: the need for standardized approaches. *Artif. Organs* **2017**, *41* (8), 778–784.

(210) Li, Z.-H.; Ji, S.-C.; Wang, Y.-Z.; Shen, X.-C.; Liang, H. Silk fibroin-based scaffolds for tissue engineering. *Front. Mater. Sci.* **2013**, *7* (3), 237–247.

(211) Ribeiro, M.; Fernandes, M. H.; Beppu, M. M.; Monteiro, F. J.; Ferraz, M. P. Silk fibroin/nanohydroxyapatite hydrogels for promoted bioactivity and osteoblastic proliferation and differentiation of human bone marrow stromal cells. *Mater. Sci. Eng., C* **2018**, *89*, 336–345.

(212) Mulligan, J. A.; Ling, L.; Leartprapun, N.; Fischbach, C.; Adie, S. G. Computational 4D-OCM for label-free imaging of collective cell invasion and force-mediated deformations in collagen. *Sci. Rep.* **2021**, *11*, 2814.

(213) Wang, L.; Chen, Z.; Yan, Y.; He, C.; Li, X. Fabrication of injectable hydrogels from silk fibroin and angiogenic peptides for vascular growth and tissue regeneration. *Chem. Eng. J.* **2021**, *418*, 129308.

(214) Wu, P.; Liu, Q.; Wang, Q.; Qian, H.; Yu, L.; Liu, B.; Li, R. Novel silk fibroin nanoparticles incorporated silk fibroin hydrogel for inhibition of cancer stem cells and tumor growth. *Int. J. Nanomed.* **2018**, *13*, 5405.

(215) Carvalho, M. R.; Maia, F. R.; Vieira, S.; Reis, R. L.; Oliveira, J. M. Tuning enzymatically crosslinked silk fibroin hydrogel properties for the development of a colorectal cancer extravasation 3D model on a chip. *Global Challenges* **2018**, *2* (5–6), 1700100.

(216) Cushing, M. C.; Anseth, K. S. Hydrogel cell cultures. *Science* **2007**, *316* (5828), 1133–1134.

(217) Peppas, N. A.; Hilt, J. Z.; Khademhosseini, A.; Langer, R. Hydrogels in biology and medicine: from molecular principles to bionanotechnology. *Adv. Mater.* **2006**, *18* (11), 1345–1360.

(218) Burdick, J. A. Cellular control in two clicks. *Nature* **2009**, *460* (7254), 469–470.

(219) DeForest, C. A.; Polizzotti, B. D.; Anseth, K. S. Sequential click reactions for synthesizing and patterning three-dimensional cell microenvironments. *Nat. Mater.* **2009**, *8* (8), 659–664.

(220) Guvendiren, M.; Burdick, J. A. Engineering synthetic hydrogel microenvironments to instruct stem cells. *Curr. Opin. Biotechnol.* **2013**, *24* (5), 841–846.

(221) Danen, E. H.; Sonnenberg, A. Erratum: Integrins in regulation of tissue development and function. J Pathol; 200:471–480. *J. Pathol.* **2003**, *201* (4), 632–641.

(222) Ruoslahti, E. The RGD story: a personal account. *Matrix Biol.* **2003**, *22* (6), 459–465.

(223) Fittkau, M.; Zilla, P.; Bezuidenhout, D.; Lutolf, M.; Human, P.; Hubbell, J.; Davies, N. The selective modulation of endothelial cell mobility on RGD peptide containing surfaces by YIGSR peptides. *Biomaterials* **2005**, *26* (2), 167–174.

(224) Sun, W.; Incitti, T.; Migliaresi, C.; Quattrone, A.; Casarosa, S.; Motta, A. Viability and neuronal differentiation of neural stem cells encapsulated in silk fibroin hydrogel functionalized with an IKVAV peptide. *J. Tissue Eng. Regen. Med.* **2017**, *11* (5), 1532–1541.

(225) Lauridsen, H. M.; Gonzalez, A. L. Biomimetic, ultrathin and elastic hydrogels regulate human neutrophil extravasation across endothelial-pericyte bilayers. *PLoS One* **2017**, *12* (2), e0171386.

(226) Klotz, B. J.; Oosterhoff, L. A.; Utomo, L.; Lim, K. S.; Vallmajo-Martin, Q.; Clevers, H.; Woodfield, T. B. F.; Rosenberg, A. J. W. P.; Malda, J.; Ehrbar, M.; Spee, B.; Gawlitta, D. A versatile biosynthetic hydrogel platform for engineering of tissue analogues. *Adv. Healthcare Mater.* **2019**, *8* (19), 1900979.

(227) Balion, Z.; Cepla, V.; Svirskiene, N.; Svirskis, G.; Druceikaite, K.; Inokaitis, H.; Rusteikaite, J.; Masilionis, I.; Stankeviciene, G.; Jelinskas, T.; Ulcinas, A.; Samanta, A.; Valiokas, R.; Jekabsone, A. Cerebellar cells self-assemble into functional organoids on synthetic, chemically crosslinked ECM-mimicking peptide hydrogels. *Biomolecules* **2020**, *10* (5), 754.

(228) Lu, P.; Takai, K.; Weaver, V. M.; Werb, Z. Extracellular matrix degradation and remodeling in development and disease. *Cold Spring Harb. Perspect. Biol.* **2011**, *3* (12), a005058.

(229) Lutolf, M.; Lauer-Fields, J.; Schmoekel, H.; Metters, A. T.; Weber, F.; Fields, G.; Hubbell, J. A. Synthetic matrix metalloproteinase-sensitive hydrogels for the conduction of tissue regeneration: engineering cell-invasion characteristics. *Proc. Natl. Acad. Sci. U. S. A.* **2003**, *100* (9), 5413–5418.

(230) Cruz-Acuña, R.; Mulero-Russe, A.; Clark, A. Y.; Zent, R.; García, A. J. Identification of matrix physicochemical properties required for renal epithelial cell tubulogenesis by using synthetic hydrogels. *J. Cell Sci.* **2019**, *132* (20), jcs226639.

(231) Jha, A. K.; Tharp, K. M.; Browne, S.; Ye, J.; Stahl, A.; Yeghiazarians, Y.; Healy, K. E. Matrix metalloproteinase-13 mediated degradation of hyaluronic acid-based matrices orchestrates stem cell engraftment through vascular integration. *Biomaterials* **2016**, *89*, 136–147.

(232) Tam, R. Y.; Smith, L. J.; Shoichet, M. S. Engineering cellular microenvironments with photo-and enzymatically responsive hydrogels: toward biomimetic 3D cell culture models. *Acc. Chem. Res.* **2017**, *50* (4), 703–713.

(233) Mao, H.; Yang, L.; Zhu, H.; Wu, L.; Ji, P.; Yang, J.; Gu, Z. Recent advances and challenges in materials for 3D bioprinting. *Prog. Nat. Sci.: Mater. Int.* **2020**, *30* (5), 618–634.

(234) Unagolla, J. M.; Jayasuriya, A. C. Hydrogel-based 3D bioprinting: A comprehensive review on cell-laden hydrogels, bioink formulations, and future perspectives. *Appl. Mater. Today* **2020**, *18*, 100479.

(235) Puperi, D. S.; Balaoing, L. R.; O'Connell, R. W.; West, J. L.; Grande-Allen, K. J. 3-Dimensional spatially organized PEG-based hydrogels for an aortic valve co-culture model. *Biomaterials* **2015**, *67*, 354−364.

(236) Kwak, H.; Shin, S.; Lee, H.; Hyun, J. Formation of a keratin layer with silk fibroin-polyethylene glycol composite hydrogel fabricated by digital light processing 3D printing. *J. Ind. Eng. Chem.* **2019**, *72*, 232−240.

(237) Kim, S. H.; Yeon, Y. K.; Lee, J. M.; Chao, J. R.; Lee, Y. J.; Seo, Y. B.; Sultan, M.; Lee, O. J.; Lee, J. S.; Yoon, S.-i. Precisely printable and biocompatible silk fibroin bioink for digital light processing 3D printing. *Nat. Commun.* **2018**, *9*, 1620.

(238) Contessi Negrini, N.; Angelova Volponi, A.; Sharpe, P. T.; Celiz, A. D. Tunable Cross-Linking and Adhesion of Gelatin Hydrogels via Bioorthogonal Click Chemistry. *ACS Biomater. Sci. Eng.* **2021**, *7* (9), 4330−4346.

(239) Kwag, H. R.; Serbo, J. V.; Korangath, P.; Sukumar, S.; Romer, L. H.; Gracias, D. H. A self-folding hydrogel in vitro model for ductal carcinoma. *Tissue Eng., Part C* **2016**, *22* (4), 398−407.

(240) Zamprogno, P.; Wuthrich, S.; Achenbach, S.; Thoma, G.; Stucki, J. D.; Hobi, N.; Schneider-Daum, N.; Lehr, C.-M.; Huwer, H.; Geiser, T.; Schmid, R. A.; Guenat, O. T. Second-generation lung-on-a-chip with an array of stretchable alveoli made with a biological membrane. *Commun. Biol.* **2021**, *4*, 168.

(241) Fan, H.; Hu, Y.; Zhang, C.; Li, X.; Lv, R.; Qin, L.; Zhu, R. Cartilage regeneration using mesenchymal stem cells and a PLGA−gelatin/chondroitin/hyaluronate hybrid scaffold. *Biomaterials* **2006**, *27* (26), 4573−4580.

(242) Lan, S.-F.; Starly, B. Alginate based 3D hydrogels as an in vitro co-culture model platform for the toxicity screening of new chemical entities. *Toxicol. Appl. Pharmacol.* **2011**, *256* (1), 62−72.

(243) Huang, D.; Liu, T.; Liao, J.; Maharjan, S.; Xie, X.; Pérez, M.; Anaya, I.; Wang, S.; Tirado Mayer, A.; Kang, Z.; et al. Reversed-engineered human alveolar lung-on-a-chip model. *Proc. Natl. Acad. Sci. U. S. A.* **2021**, *118* (19), e2016146118.

(244) Ruprecht, V.; Monzo, P.; Ravasio, A.; Yue, Z.; Makhija, E.; Strale, P. O.; Gauthier, N.; Shivashankar, G.; Studer, V.; Albiges-Rizo, C. How cells respond to environmental cues−insights from bio-functionalized substrates. *J. Cell Sci.* **2017**, *130* (1), 51−61.

(245) Ji, S.; Almeida, E.; Guvendiren, M. 3D bioprinting of complex channels within cell-laden hydrogels. *Acta Biomater.* **2019**, *95*, 214−224.

(246) Yang, J.; Zhang, Y. S.; Yue, K.; Khademhosseini, A. Cell-laden hydrogels for osteochondral and cartilage tissue engineering. *Acta Biomater.* **2017**, *57*, 1−25.

(247) Ortiz-Cárdenas, J. E.; Zatorski, J. M.; Arneja, A.; Montalbine, A. N.; Munson, J. M.; Luckey, C. J.; Pompano, R. R. Towards spatially-organized organs-on-chip: Photopatterning cell-laden thiol-ene and methacryloyl hydrogels in a microfluidic device. *Organs-on-a-Chip* **2022**, *4*, 100018.

(248) Abdallah, M.; Martin, M.; El Tahchi, M. R.; Balme, S.; Faour, W. H.; Varga, B.; Cloitre, T.; Pall, O.; Cuisinier, F. J. G.; Gergely, C.; Bassil, M. J.; Bechelany, M. Influence of Hydrolyzed Polyacrylamide Hydrogel Stiffness on Podocyte Morphology, Phenotype, and Mechanical Properties. *ACS Appl. Mater. Interfaces* **2019**, *11* (36), 32623−32632.

(249) Ramadhan, W.; Kagawa, G.; Hamada, Y.; Moriyama, K.; Wakabayashi, R.; Minamihata, K.; Goto, M.; Kamiya, N. Enzymatically prepared dual functionalized hydrogels with gelatin and heparin to facilitate cellular attachment and proliferation. *ACS Appl. Bio Mater.* **2019**, *2* (6), 2600−2609.

(250) Barros da Silva, P.; Coelho, M.; Bidarra, S. J.; Neves, S. C.; Barrias, C. C. Reshaping in vitro models of breast tissue: integration of stromal and parenchymal compartments in 3D printed hydrogels. *Front. Bioeng. Biotechnol.* **2020**, *8*, 494.

(251) Kumar, P.; Ciftci, S.; Barthes, J.; Knopf-Marques, H.; Muller, C. B.; Debry, C.; Vrana, N. E.; Ghaemmaghami, A. M. A composite Gelatin/hyaluronic acid hydrogel as an ECM mimic for developing mesenchymal stem cell-derived epithelial tissue patches. *J. Tissue Eng. Regen. Med.* **2020**, *14* (1), 45−57.

(252) Tang, Y.; Cai, X.; Xiang, Y.; Zhao, Y.; Zhang, X.; Wu, Z. Cross-linked antifouling polysaccharide hydrogel coating as extracellular matrix mimics for wound healing. *J. Mater. Chem. B* **2017**, *5* (16), 2989−2999.

(253) Brown, T. E.; Carberry, B. J.; Worrell, B. T.; Dudaryeva, O. Y.; McBride, M. K.; Bowman, C. N.; Anseth, K. S. Photopolymerized dynamic hydrogels with tunable viscoelastic properties through thioester exchange. *Biomaterials* **2018**, *178*, 496−503.

(254) Loessner, D.; Meinert, C.; Kaemmerer, E.; Martine, L. C.; Yue, K.; Levett, P. A.; Klein, T. J.; Melchels, F. P.; Khademhosseini, A.; Hutmacher, D. W. Functionalization, preparation and use of cell-laden gelatin methacryloyl−based hydrogels as modular tissue culture platforms. *Nat. Protoc.* **2016**, *11* (4), 727.

(255) Beamish, J. A.; Chen, E.; Putnam, A. J. Engineered extracellular matrices with controlled mechanics modulate renal proximal tubular cell epithelialization. *PLoS One* **2017**, *12* (7), e0181085.

(256) Bian, S.; Cai, H.; Cui, Y.; He, M.; Cao, W.; Chen, X.; Sun, Y.; Liang, J.; Fan, Y.; Zhang, X. Temperature and ion dual responsive biphenyl-dipeptide supramolecular hydrogels as extracellular matrix mimic-scaffolds for cell culture applications. *J. Mater. Chem. B* **2017**, *5* (20), 3667−3674.

(257) Capella, V.; Rivero, R. E.; Liaudat, A. C.; Ibarra, L. E.; Roma, D. A.; Alustiza, F.; Manas, F.; Barbero, C. A.; Bosch, P.; Rivarola, C. R.; Rodriguez, N. Cytotoxicity and bioadhesive properties of poly-N-isopropylacrylamide hydrogel. *Heliyon* **2019**, *5* (4), e01474.

(258) Montalbano, G.; Toumpaniari, S.; Popov, A.; Duan, P.; Chen, J.; Dalgarno, K.; Scott, W., III; Ferreira, A. Synthesis of bioinspired collagen/alginate/fibrin based hydrogels for soft tissue engineering. *Mater. Sci. Eng., C* **2018**, *91*, 236−246.

(259) Geissler, S. A.; Sabin, A. L.; Besser, R. R.; Gooden, O. M.; Shirk, B. D.; Nguyen, Q. M.; Khaing, Z. Z.; Schmidt, C. E. Biomimetic hydrogels direct spinal progenitor cell differentiation and promote functional recovery after spinal cord injury. *J. Neural Eng.* **2018**, *15* (2), 025004.

(260) Xu, W.; Qian, J.; Zhang, Y.; Suo, A.; Cui, N.; Wang, J.; Yao, Y.; Wang, H. A double-network poly (Nε-acryloyl L-lysine)/hyaluronic acid hydrogel as a mimic of the breast tumor microenvironment. *Acta Biomater.* **2016**, *33*, 131−141.

(261) Negrini, N. C.; Bonnetier, M.; Giatsidis, G.; Orgill, D. P.; Farè, S.; Marelli, B. Tissue-mimicking gelatin scaffolds by alginate sacrificial templates for adipose tissue engineering. *Acta Biomater.* **2019**, *87*, 61−75.

(262) Li, D.; Xia, Y. Electrospinning of nanofibers: reinventing the wheel? *Adv. Mater.* **2004**, *16* (14), 1151−1170.

(263) Rogina, A. Electrospinning process: Versatile preparation method for biodegradable and natural polymers and biocomposite systems applied in tissue engineering and drug delivery. *Appl. Surf. Sci.* **2014**, *296*, 221−230.

(264) Rho, K. S.; Jeong, L.; Lee, G.; Seo, B.-M.; Park, Y. J.; Hong, S.-D.; Roh, S.; Cho, J. J.; Park, W. H.; Min, B.-M. Electrospinning of collagen nanofibers: effects on the behavior of normal human keratinocytes and early-stage wound healing. *Biomaterials* **2006**, *27* (8), 1452−1461.

(265) Mariotti, M.; Rogowska-Wrzesinska, A.; Hägglund, P.; Davies, M. J. Cross-linking and modification of fibronectin by peroxynitrous acid: Mapping and quantification of damage provides a new model for domain interactions. *J. Biol. Chem.* **2021**, *296*, 100360.

(266) Neal, R. A.; McClugage, S. G., III; Link, M. C.; Sefcik, L. S.; Ogle, R. C.; Botchwey, E. A. Laminin nanofiber meshes that mimic morphological properties and bioactivity of basement membranes. *Tissue Eng., Part C* **2009**, *15* (1), 11−21.

(267) Kleinman, H. K.; McGarvey, M. L.; Hassell, J. R.; Martin, G. R. Formation of a supramolecular complex is involved in the reconstitution of basement membrane components. *Biochemistry* **1983**, *22* (21), 4969−4974.

(268) Kakade, M. V.; Givens, S.; Gardner, K.; Lee, K. H.; Chase, D. B.; Rabolt, J. F. Electric field induced orientation of polymer chains in macroscopically aligned electrospun polymer nanofibers. *J. Am. Chem. Soc.* **2007**, *129* (10), 2777−2782.

(269) Wondimu, Z.; Gorfu, G.; Kawataki, T.; Smirnov, S.; Yurchenco, P.; Tryggvason, K.; Patarroyo, M. Characterization of commercial laminin preparations from human placenta in comparison to recombinant laminins 2 ($\alpha2\beta1\gamma1$), 8 ($\alpha4\beta1\gamma1$), 10 ($\alpha5\beta1\gamma1$). *Matrix Biol.* **2006**, *25* (2), 89−93.

(270) Jin, H.-J.; Chen, J.; Karageorgiou, V.; Altman, G. H.; Kaplan, D. L. Human bone marrow stromal cell responses on electrospun silk fibroin mats. *Biomaterials* **2004**, *25* (6), 1039−1047.

(271) Ko, E.; Lee, J. S.; Kim, H.; Yang, S. Y.; Yang, D.; Yang, K.; Lee, J.; Shin, J.; Yang, H. S.; Ryu, W.; Cho, S.-W. Electrospun silk fibroin nanofibrous scaffolds with two-stage hydroxyapatite functionalization for enhancing the osteogenic differentiation of human adipose-derived mesenchymal stem cells. *ACS Appl. Mater. Interfaces* **2018**, *10* (9), 7614−7625.

(272) Liu, W.; Li, Z.; Zheng, L.; Zhang, X.; Liu, P.; Yang, T.; Han, B. Electrospun fibrous silk fibroin/poly (L-lactic acid) scaffold for cartilage tissue engineering. *Tissue Eng. Regener. Med.* **2016**, *13* (5), 516−526.

(273) Bulysheva, A. A.; Bowlin, G. L.; Klingelhutz, A. J.; Yeudall, W. A. Low-temperature electrospun silk scaffold for in vitro mucosal modeling. *J. Biomed. Mater. Res., Part A* **2012**, *100A* (3), 757−767.

(274) Kim, B. S.; Park, K. E.; Kim, M. H.; You, H. K.; Lee, J.; Park, W. H. Effect of nanofiber content on bone regeneration of silk fibroin/poly (ε-caprolactone) nano/microfibrous composite scaffolds. *Int. J. Nanomed.* **2015**, *10*, 485.

(275) Tanzi, M. C.; Marcolin, C.; Draghi, L.; Farè, S. 2D and 3D Electrospun Silk Fibroin Gelatin Coatings to Improve Scaffold Performances in Cardiovascular Applications. *Materials Proceedings* **2020**, *2* (1), 20.

(276) Xue, C.; Zhu, H.; Tan, D.; Ren, H.; Gu, X.; Zhao, Y.; Zhang, P.; Sun, Z.; Yang, Y.; Gu, J.; Gu, Y.; Gu, X. Electrospun silk fibroin-based neural scaffold for bridging a long sciatic nerve gap in dogs. *J. Tissue Eng. Regen. Med.* **2018**, *12* (2), e1143−e1153.

(277) Mou, X.; Shah, J.; Bhattacharya, R.; Kalejaiye, T. D.; Sun, B.; Hsu, P.-C.; Musah, S. A Biomimetic Electrospun Membrane Supports the Differentiation and Maturation of Kidney Epithelium from Human Stem Cells. *Bioengineering* **2022**, *9* (5), 188.

(278) Cheng, G.; Dai, J.; Dai, J.; Wang, H.; Chen, S.; liu, Y.; Liu, X.; Li, X.; Zhou, X.; Deng, H.; Li, Z. Extracellular matrix imitation utilizing nanofibers-embedded biomimetic scaffolds for facilitating cartilage regeneration. *Chem. Eng. J.* **2021**, *410*, 128379.

(279) Chan, A. H. P.; Filipe, E. C.; Tan, R. P.; Santos, M.; Yang, N.; Hung, J.; Feng, J.; Nazir, S.; Benn, A. J.; Ng, M. K. C.; Rnjak-Kovacina, J.; Wise, S. G. Altered processing enhances the efficacy of small-diameter silk fibroin vascular grafts. *Sci. Rep.* **2019**, *9*, 17461.

(280) Li, G.; Chen, K.; You, D.; Xia, M.; Li, W.; Fan, S.; Chai, R.; Zhang, Y.; Li, H.; Sun, S. Laminin-coated electrospun regenerated silk fibroin mats promote neural progenitor cell proliferation, differentiation, and survival in vitro. *Front. Bioeng. Biotechnol.* **2019**, *7*, 190.

(281) Liu, Q.; Ying, G.; Jiang, N.; Yetisen, A. K.; Yao, D.; Xie, X.; Fan, Y.; Liu, H. Three-dimensional silk fibroin microsphere-nanofiber scaffolds for vascular tissue engineering. *Medicine in Novel Technology and Devices* **2021**, *9*, 100051.

(282) Sobreiro-Almeida, R.; Fonseca, D. R.; Neves, N. M. Extracellular matrix electrospun membranes for mimicking natural renal filtration barriers. *Mater. Sci. Eng., C* **2019**, *103*, 109866.

(283) Bye, F. J.; Bullock, A. J.; Singh, R.; Sefat, F.; Roman, S.; MacNeil, S. Development of a basement membrane substitute incorporated into an electrospun scaffold for 3D skin tissue engineering. *J. Biomater. Tissue Eng.* **2014**, *4* (9), 686−692.

(284) Huang, Z.-M.; Zhang, Y.-Z.; Kotaki, M.; Ramakrishna, S. A review on polymer nanofibers by electrospinning and their applications in nanocomposites. *Compos. Sci. Technol.* **2003**, *63* (15), 2223−2253.

(285) Kim, H. S.; Yoo, H. S. MMPs-responsive release of DNA from electrospun nanofibrous matrix for local gene therapy: in vitro and in vivo evaluation. *J. Controlled Release* **2010**, *145* (3), 264−271.

(286) Sundararaghavan, H. G.; Metter, R. B.; Burdick, J. A. Electrospun fibrous scaffolds with multiscale and photopatterned porosity. *Macromol. Biosci.* **2010**, *10* (3), 265−270.

(287) Khodamoradi, M.; Eskandari, M.; Keshvari, H.; Zarei, R. An electro-conductive hybrid scaffold as an artificial Bruch's membrane. *Mater. Sci. Eng., C* **2021**, *126*, 112180.

(288) Wade, R. J.; Bassin, E. J.; Rodell, C. B.; Burdick, J. A. Protease-degradable electrospun fibrous hydrogels. *Nat. Commun.* **2015**, *6*, 6639.

(289) Paulsson, M.; Fujiwara, S.; Dziadek, M.; Timpl, R.; Pejler, G.; Bäckström, G.; Lindahl, U.; Engel, J. *Structure and function of basement membrane proteoglycans*, Ciba Foundation Symposium 124-Functions of the Proteoglycans: Functions of the Proteoglycans: Ciba Foundation Symposium 124, Wiley Online Library: 2007; pp 189−203.

(290) Song, J.; Zhu, G.; Gao, H.; Wang, L.; Li, N.; Shi, X.; Wang, Y. Origami meets electrospinning: a new strategy for 3D nanofiber scaffolds. *Bio-Des. Manuf.* **2018**, *1* (4), 254−264.

(291) Wang, L.; Wang, B.; Ahmad, Z.; Li, J.-S.; Chang, M.-W. Dual rotation centrifugal electrospinning: a novel approach to engineer multi-directional and layered fiber composite matrices. *Drug Delivery Transl. Res.* **2019**, *9* (1), 204−214.

(292) Dohle, E.; Singh, S.; Nishigushi, A.; Fischer, T.; Wessling, M.; Möller, M.; Sader, R.; Kasper, J.; Ghanaati, S.; Kirkpatrick, C. J. Human Co-and triple-culture model of the alveolar-capillary barrier on a basement membrane mimic. *Tissue Eng., Part C* **2018**, *24* (9), 495−503.

(293) Bhardwaj, N.; Kundu, S. C. Electrospinning: a fascinating fiber fabrication technique. *Biotechnol. Adv.* **2010**, *28* (3), 325−347.

(294) Madurantakam, P. A.; Rodriguez, I. A.; Beckman, M. J.; Simpson, D. G.; Bowlin, G. L. Evaluation of biological activity of bone morphogenetic proteins on exposure to commonly used electrospinning solvents. *J. Bioact. Compat. Polym.* **2011**, *26* (6), 578−589.

(295) Fee, T.; Surianarayanan, S.; Downs, C.; Zhou, Y.; Berry, J. Nanofiber alignment regulates NIH3T3 cell orientation and cytoskeletal gene expression on electrospun PCL+ gelatin nanofibers. *PLoS One* **2016**, *11* (5), e0154806.

(296) Zhou, H.; Wang, H.; Niu, H.; Lin, T. Electrospun fibrous membranes with super-large-strain electric superhydrophobicity. *Sci. Rep.* **2015**, *5*, 15863.

(297) Rhyou, J.; Youn, J.; Eom, S.; Kim, D. S. Facile Fabrication of Electrospun Nanofiber Membrane-Integrated PDMS Microfluidic Chip via Silver Nanowires-Uncured PDMS Adhesive Layer. *ACS Macro Lett.* **2021**, *10* (7), 965−970.

(298) Neal, R. A.; McClugage, S. G.; Link, M. C.; Sefcik, L. S.; Ogle, R. C.; Botchwey, E. A. Laminin Nanofiber Meshes That Mimic Morphological Properties and Bioactivity of Basement Membranes. *Tissue Eng., Part C* **2009**, *15* (1), 11−21.

(299) Ma, Z.; Kotaki, M.; Yong, T.; He, W.; Ramakrishna, S. Surface engineering of electrospun polyethylene terephthalate (PET) nanofibers towards development of a new material for blood vessel engineering. *Biomaterials* **2005**, *26* (15), 2527−2536.

(300) Lv, J.; Chen, L.; Zhu, Y.; Hou, L.; Liu, Y. Promoting epithelium regeneration for esophageal tissue engineering through basement membrane reconstitution. *ACS Appl. Mater. Interfaces* **2014**, *6* (7), 4954−4964.

(301) Rossi, A.; Wistlich, L.; Heffels, K. H.; Walles, H.; Groll, J. Isotropic Versus Bipolar Functionalized Biomimetic Artificial Basement Membranes and Their Evaluation in Long-Term Human Cell Co-Culture. *Adv. Healthcare Mater.* **2016**, *5* (15), 1939−1948.

(302) Rajabi, M.; Firouzi, M.; Hassannejad, Z.; Haririan, I.; Zahedi, P. Fabrication and characterization of electrospun laminin-functionalized silk fibroin/poly (ethylene oxide) nanofibrous scaffolds for peripheral nerve regeneration. *J. Biomed. Mater. Res. B Appl. Biomater.* **2018**, *106* (4), 1595−1604.

(303) Ghasemi-Mobarakeh, L.; Prabhakaran, M. P.; Morshed, M.; Nasr-Esfahani, M. H.; Ramakrishna, S. Bio-functionalized PCL nanofibrous scaffolds for nerve tissue engineering. *Mater. Sci. Eng., C* **2010**, *30* (8), 1129−1136.

(304) Aslani, S.; Kabiri, M.; Kehtari, M.; Hanaee-Ahvaz, H. Vascular tissue engineering: Fabrication and characterization of acetylsalicylic acid-loaded electrospun scaffolds coated with amniotic membrane lysate. *J. Cell. Physiol.* **2019**, *234* (9), 16080−16096.

(305) Foraida, Z. I.; Kamaldinov, T.; Nelson, D. A.; Larsen, M.; Castracane, J. Elastin-PLGA hybrid electrospun nanofiber scaffolds for salivary epithelial cell self-organization and polarization. *Acta Biomater.* **2017**, *62*, 116−127.

(306) Pensabene, V.; Crowder, S. W.; Balikov, D. A.; Lee, J. B.; Sung, H.-J. *Optimization of electrospun fibrous membranes for in vitro modeling of blood-brain barrier*, 2016 38th Annual International Conference of the IEEE Engineering in Medicine and Biology Society (EMBC), IEEE: 2016; pp 125−128.

(307) Pazhanimala, S. K.; Vllasaliu, D.; Raimi-Abraham, B. T. Electrospun nanometer to micrometer scale biomimetic synthetic membrane scaffolds in drug delivery and tissue engineering: a review. *Appl. Sci.* **2019**, *9* (5), 910.

(308) Koetting, M. C.; Peters, J. T.; Steichen, S. D.; Peppas, N. A. Stimulus-responsive hydrogels: Theory, modern advances, and applications. *Mater. Sci. Eng. R Rep.* **2015**, *93*, 1−49.

(309) Huang, G.; Li, F.; Zhao, X.; Ma, Y.; Li, Y.; Lin, M.; Jin, G.; Lu, T. J.; Genin, G. M.; Xu, F. Functional and biomimetic materials for engineering of the three-dimensional cell microenvironment. *Chem. Rev.* **2017**, *117* (20), 12764−12850.

(310) Keshvardoostchokami, M.; Majidi, S. S.; Huo, P.; Ramachandran, R.; Chen, M.; Liu, B. Electrospun nanofibers of natural and synthetic polymers as artificial extracellular matrix for tissue engineering. *Nanomaterials* **2021**, *11* (1), 21.

(311) Nicolas, J.; Magli, S.; Rabbachin, L.; Sampaolesi, S.; Nicotra, F.; Russo, L. 3D extracellular matrix mimics: fundamental concepts and role of materials chemistry to influence stem cell fate. *Biomacromolecules* **2020**, *21* (6), 1968−1994.

(312) Bracaglia, L. G.; Smith, B. T.; Watson, E.; Arumugasaamy, N.; Mikos, A. G.; Fisher, J. P. 3D printing for the design and fabrication of polymer-based gradient scaffolds. *Acta Biomater.* **2017**, *56*, 3−13.

(313) Jo, H.; Yoon, M.; Gajendiran, M.; Kim, K. Recent strategies in fabrication of gradient hydrogels for tissue engineering applications. *Macromol. Biosci.* **2020**, *20* (3), 1900300.

(314) Malandrino, A.; Mak, M.; Kamm, R. D.; Moeendarbary, E. Complex mechanics of the heterogeneous extracellular matrix in cancer. *Extreme Mechanics Letters* **2018**, *21*, 25−34.

(315) Brassard, J. A.; Lutolf, M. P. Engineering stem cell self-organization to build better organoids. *Cell stem cell* **2019**, *24* (6), 860−876.